Lecture *Notes:*
Accurate Solutions of Radiative Transfer Problems

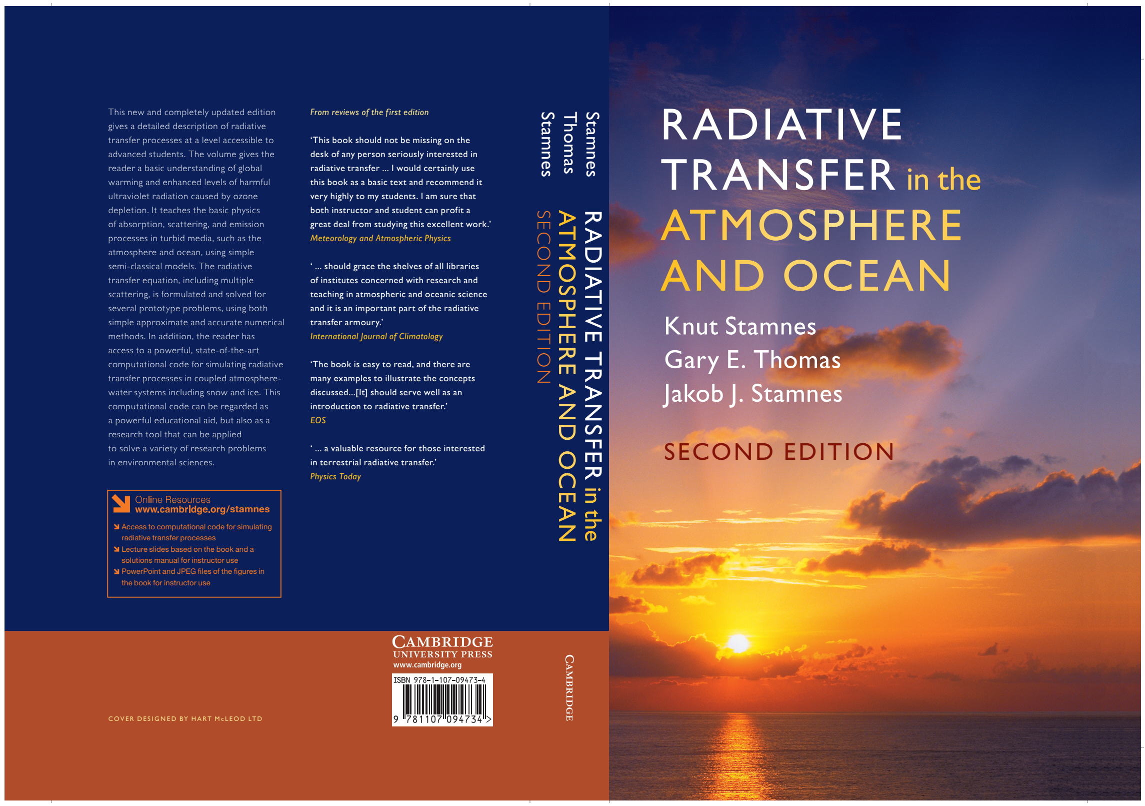

Based primarily on Chapter 9 in K. Stamnes, G. E. Thomas, and J. J. Stamnes, Radiative Transfer in the Atmosphere and Ocean, Cambridge University Press, 2017.

A Tutorial Review of the DISORT Formulation

Motivation: Why Do We Study Radiative Transfer?

One reason is illustrated in Figure 1:

- **Sunlight passing through the atmosphere interacts with molecules and aerosol particles.**
- **A fraction of the light is transmitted into the ocean where it interacts with pure water as well as embedded (algal and non-algal) particles.**
- Some of this light is scattered upwards, transmitted back into the air and then to the top of the atmosphere, where it is measured by an instrument deployed on a satellite (Earth-orbiting or geostationary).
- **Such measurements are carried out at several selected wavelengths in the UV, visible and infrared spectral region.**
- **What can we learn about the atmosphere and the ocean from such measurements of "ocean color"?**

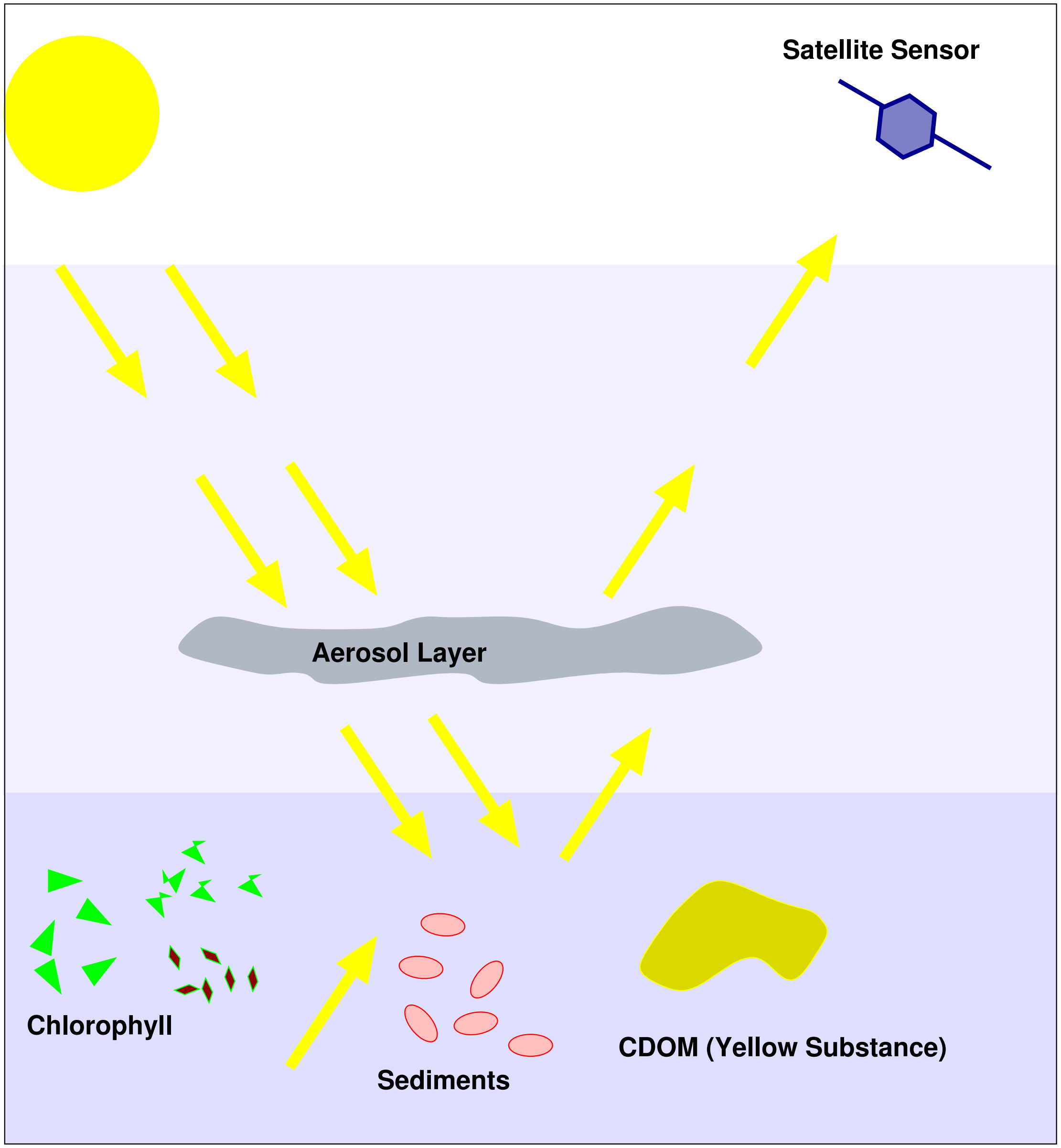

Figure 1: **A schematic illustration showing aspects of the retrieval problem.**

Generic Radiative Transfer Equation and Formal Solution (1)

Ignoring time-dependence, we may write the differential equation of radiative transfer as:

$$\hat{\Omega} \cdot \nabla I(\nu, s, \hat{\Omega}) = \frac{dI(\nu, s, \hat{\Omega})}{ds} = -k(\nu, s) I(\nu, s, \hat{\Omega}) + S(\nu, s, \hat{\Omega}) \tag{1}$$

- $I(\nu, s, \hat{\Omega})$ is the monochromatic radiance in direction $\hat{\Omega}$ at frequency ν and position s.

The extinction coefficient $k(\nu, s)$ is:

- the sum of the scattering coefficient $\sigma(\nu, s)$ and the absorption coefficient $\alpha(\nu, s)$, i.e., $k(\nu, s) = \sigma(\nu, s) + \alpha(\nu, s)$.
- The operator $\hat{\Omega} \cdot \nabla$ indicates the rate of change of the radiance in the direction $\hat{\Omega}$.

Generic Radiative Transfer Equation and Formal Solution (2)

In local thermodynamic equilibrium (LTE) the source function becomes:

$$S(\nu, s, \hat{\Omega}) = \alpha(\nu, s)B[\nu, T(s)] + \frac{\sigma(\nu, s)}{4\pi} \int_{4\pi} d\hat{\Omega}' \, p(\nu, s, \hat{\Omega}', \hat{\Omega}) I(\nu, s, \hat{\Omega}') \tag{2}$$

- $B[\nu, T(s)]$ is the Planck function, $T(s)$ is the temperature, and $p(\nu, s, \hat{\Omega}', \hat{\Omega})$ is the scattering phase function.

We introduce the dimensionless differential optical path:

- $$d\tau(\nu, s) = \sum_i [\alpha_i(\nu, s) + \sigma_i(\nu, s)] ds = [\alpha(\nu, s) + \sigma(\nu, s)] ds = k(\nu, s) ds \tag{3}$$

Generic Radiative Transfer Equation and Formal Solution (3)

Here $\alpha_i(\nu, s)$ and $\sigma_i(\nu, s)$ are the absorption and scattering coefficients of the i^{th} radiatively significant species, and:

- $\alpha(\nu, s)$ and $\sigma(\nu, s)$ are the total absorption and scattering coefficients with units $[\mathrm{m}^{-1}]$.

Defining the single-scattering albedo:

- $$\varpi(\nu, \tau) \equiv \sigma(\nu, \tau)/[\sigma(\nu, \tau) + \alpha(\nu, \tau)] \tag{4}$$

we may rewrite Eq. 1 as follows:

$$\boxed{\frac{dI(\nu, \tau, \hat{\Omega})}{d\tau} = -I(\nu, \tau, \hat{\Omega}) + S(\nu, \tau, \hat{\Omega}). \tag{5}}$$

Generic Radiative Transfer Equation and Formal Solution (4)

The dependence of τ on s and ν has been suppressed to simplify the notation, and the source function is:

$$S(\nu,\tau,\hat{\Omega}) = [1-\varpi(\nu,\tau)]B[\nu,T(\tau)] + \frac{\varpi(\nu,\tau)}{4\pi}\int_{4\pi} d\omega'\, p(\nu,\tau,\hat{\Omega}',\hat{\Omega})I(\nu,\tau,\hat{\Omega}'). \quad (6)$$

Equation 5:

$$\frac{dI(\nu,\tau,\hat{\Omega})}{d\tau} = -I(\nu,\tau,\hat{\Omega}) + S(\nu,\tau,\hat{\Omega})$$

illustrates that if we know the source function, $S(\nu,\tau,\hat{\Omega})$, then the radiance emerging in direction $\hat{\Omega}$ from an optical path originating at point s_1 and ending at point s_2 is obtained by integration:

$$\begin{aligned} I[\nu,\tau(s_2),\hat{\Omega}] &= \qquad\qquad (7) \\ &= I[\nu,\tau(s_1),\hat{\Omega}]e^{-[\tau(s_2)-\tau(s_1)]} + \int_{\tau(s_1)}^{\tau(s_2)} dt S(\nu,t(s),\hat{\Omega})e^{-[\tau(s_2)-t(s)]}. \end{aligned}$$

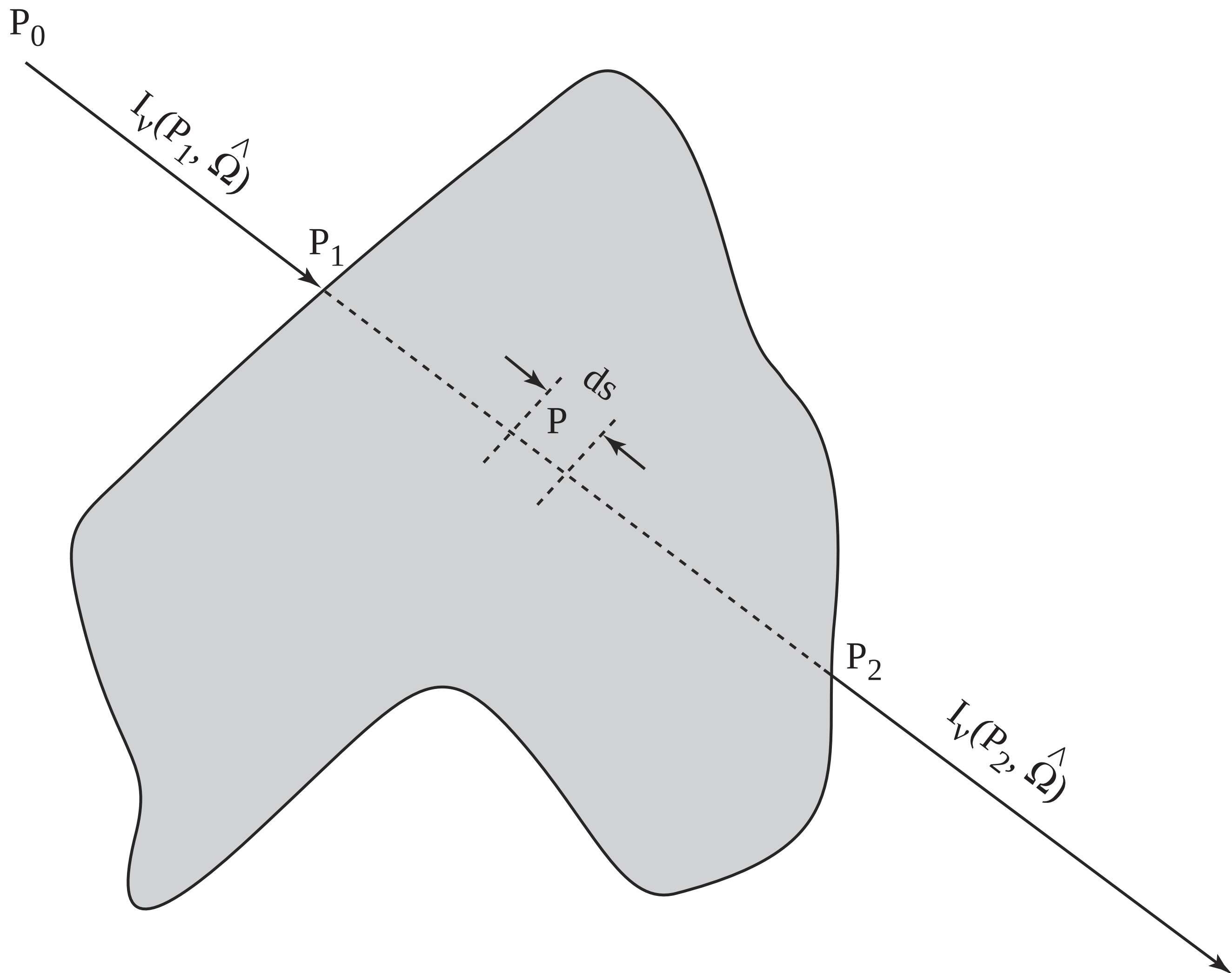

Figure 2: **A beam of radiation is incident on an absorbing/emitting region at the boundary point P_1. It is attenuated along the path P_1P_2, and emerges at the point P_2. The propagation direction of the beam is denoted by $\hat{\Omega}$. In addition, multiple scattering and thermal emission adds to the beam at all points within the medium.**

Generic Radiative Transfer Equation and Formal Solution (5)

Equation 7:

$$I[\nu, \tau(s_2), \hat{\Omega}] =$$
$$= I[\nu, \tau(s_1), \hat{\Omega}]e^{-[\tau(s_2)-\tau(s_1)]} + \int_{\tau(s_1)}^{\tau(s_2)} dt S(\nu, t(s), \hat{\Omega})e^{-[\tau(s_2)-t(s)]}$$

shows that *knowledge of the source function* is the *key to predicting the radiance*. In the absence of sources due to multiple scattering and thermal emission Eq. 7 becomes:

- $$I[\nu, \tau(s_2), \hat{\Omega}] = I[\nu, \tau(s_1), \hat{\Omega}]e^{-[\tau(s_2)-\tau(s_1)]} \quad \longleftarrow \quad \text{Beer's law} \tag{8}$$

describing *exponential beam attenuation* along the optical path between point s_1 and point s_2.

Formulation of the 1-D forward problem including multiple scattering and surface effects (1)

In general, multiple scattering, absorption, and thermal emission as well as solar forcing may be important, BUT

In the absence of *horizontally inhomogeneous* cloud and aerosol particles in the atmosphere, and hydrosols in the water:

- a *plane-parallel* (slab) or one-dimensional (1-D) geometry is appropriate in both the atmosphere and the ocean because gravity forces a density stratification.

It is common practice to measure the *optical depth* along the vertical direction downward from the "top" of the medium (see Fig. 3).

Thus, we define the *vertical* optical depth in terms of the slant optical depth $\tau(\nu, s)$ (see Eq. 3) as follows:

$$\tau(\nu, z) \equiv \int_z^\infty dz'\, k(\nu, z') \equiv \tau(\nu, s)/\mu.$$

Here z is the vertical co-ordinate, $u = \cos\theta$, $\mu = |u|$, and θ is the polar angle or the solar zenith angle ($\theta = \theta_0$, see Fig. 3). Thus:

- for an arbitrary slant path through the plane-parallel medium we have $d\tau(\nu, s) = -k(\nu, z)dz/\mu = -d\tau(\nu, z)/\mu$.

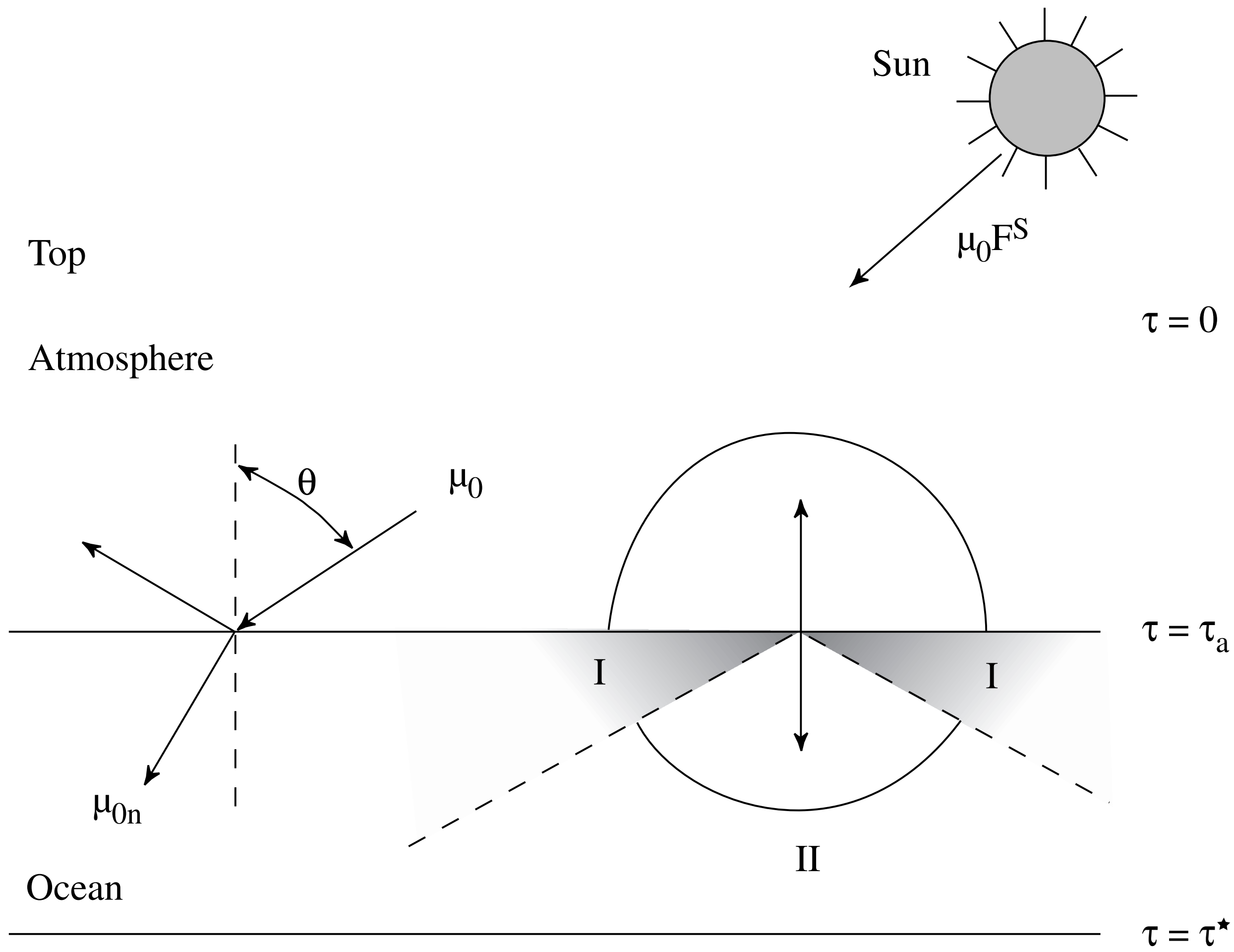

Figure 3: **Schematic illustration of two adjacent media with a flat interface such as the atmosphere overlying a calm ocean. Because the atmosphere has a different index of refraction ($m_r \approx 1$) than the ocean ($m_r \approx 1.34$), radiation distributed over 2π sr in the atmosphere will be confined to a cone less than 2π sr in the ocean (region II). Radiation in the ocean within region I will be totally reflected when striking the interface from below.**

Formulation of the 1-D forward problem (3)

Definitions:

$$d\tau = -[\alpha(z) + \sigma(z)]\,dz \quad \textbf{differential vertical optical depth} \tag{9}$$

$$\alpha(z) = \textbf{absorption coefficient} \;\; [\mathrm{m}^{-1}] \tag{10}$$

$$\sigma(z) = \textbf{scattering coefficient} \;\; [\mathrm{m}^{-1}] \tag{11}$$

$$\varpi(z) = \frac{\sigma(z)}{\alpha(z) + \sigma(z)} \quad \textbf{single – scattering albedo} \tag{12}$$

$$\alpha(z) \equiv \sum_i \alpha^i(z) = \sum_i n^i\,\alpha_n^i\,; \qquad \sigma(z) \equiv \sum_i \sigma^i(z) = \sum_i n_i\,\sigma_n^i \tag{13}$$

$$\alpha_n^i = \textbf{absorption cross section} \;\; [\mathrm{m}^2] \tag{14}$$

$$\sigma_n^i = \textbf{scattering cross section} \;\; [\mathrm{m}^2] \tag{15}$$

$$n_i = \textbf{concentration of } i^{\mathrm{th}} \textbf{ species} \;\; [\mathrm{m}^{-3}] \tag{16}$$

Scattering phase function (normalized angular scattering cross section):

$$p(\tau, \cos\Theta) = p(\tau, u', \phi'; u, \phi) = \frac{\sum_i \;\sigma^i(\tau, cos\Theta)}{\sum_i \int_{4\pi} d\;cos\Theta\;\sigma^i(\tau, cos\Theta)/4\pi} = \frac{\sum_i \;\sigma^i(\tau, cos\Theta)}{\sum_i \;\sigma^i(\tau)} = \frac{\sigma(\tau, cos\Theta)}{\sigma(\tau)} \tag{17}$$

$$\Theta = \textbf{scattering angle} \tag{18}$$

$$(\theta', \phi') = \textbf{polar and azimuthal angles } \textit{prior to} \textbf{ scattering} \tag{19}$$

$$(\theta, \phi) = \textbf{polar and azimuthal angles } \textit{after} \textbf{ scattering} \tag{20}$$

These angles are related through the cosine law of spherical geometry:

$$\cos\;\Theta = \cos\;\theta'\;\cos\theta + \sin\;\theta'\;\sin\;\theta\;\cos(\phi' - \phi). \tag{21}$$

Formulation of the 1-D forward problem (4)

Solar radiation penetrating the atmosphere and the underlying surface medium consists of a *direct* and a *diffuse* component.

For a 1-D medium the direct (solar) component (Eq. 8) becomes:

- $$I_{\rm sol}(\tau, u, \phi) = F^{\rm s}\delta(u - \mu_0)\delta(\phi - \phi_0)e^{-\tau/\mu_0}. \qquad (22)$$

Here $\tau = \tau(z)$ is the vertical optical depth, $F^{\rm s}$ is the solar irradiance (normal to the solar beam) incident at the TOA in direction (θ_0, ϕ_0).

Note that:

- the product of the δ-functions in Eq. 22 has units [sr^{-1}]. Thus $I_{\rm sol}$ *is a radiance* with units [W·m^{-2}· sr^{-1}], while $F^{\rm s}$ *is an irradiance* with units [W· m^{-2}].

In the 1-D case we assume that:

- the atmosphere as well as the underlying surface consist of slabs separated by a smooth, flat interface.

Formulation of the 1-D forward problem (5)

In such a stratified medium the *integro-differential* equation of radiative transfer (Eq. 5) describing the transport of *diffuse* radiation may be written as two coupled equations:

$$\pm\mu \frac{dI^{\pm}(\tau,\mu,\phi)}{d\tau} = I^{\pm}(\tau,\mu,\phi) - S^{\pm}(\tau,\mu,\phi) \tag{23}$$

where $I^{\pm}(\tau,\mu,\phi) \equiv I(\tau,\pm\mu,\phi)$ denotes the *diffuse* radiance at optical depth τ, in directions $(\pm\mu,\phi)$.

The source function $S^{\pm}(\tau,\mu,\phi) \equiv S(\tau,\pm\mu,\phi)$ consists of three terms:

$$S^{\pm}(\tau,\mu,\phi) = S_{\rm TH}(\tau) + S^{\pm}_{\rm MS}(\tau,\mu,\phi) + S^{*\pm}(\tau,\mu,\phi). \tag{24}$$

The first term is the (isotropic) contribution from thermal radiation:

$$S_{\rm TH}(\tau) = [1-\varpi(\tau)]B[T(\tau)]. \tag{25}$$

The second term $S^{\pm}_{\rm MS}(\tau,\mu,\phi)$ is due to multiple scattering.

Formulation of the 1-D forward problem (6)

We rewrite it as:

$$\begin{aligned} S^{\pm}_{\rm MS}(\tau,\mu,\phi) &= \frac{\varpi(\tau)}{4\pi} \int_0^{2\pi} d\phi' \int_{-1}^{1} du'\ p(\tau,u',\phi';\pm\mu,\phi) I(\tau,u',\phi') \qquad (26) \\ &= \frac{\varpi(\tau)}{4\pi} \int_0^{2\pi} d\phi' \{ \int_0^1 d\mu' p(\tau,-\mu',\phi';\pm\mu,\phi) I^-(\tau,\mu',\phi') \\ &+ \int_0^1 d\mu' p(\tau,\mu',\phi';\pm\mu,\phi) I^+(\tau,\mu',\phi') \} \end{aligned}$$

to emphasize more clearly the **coupling** between the downward radiance $I^+(\tau,\mu,\phi)$ and upward radiance $I^-(\tau,\mu,\phi)$ implicit in Eqs. 23:

$$\pm\mu \frac{dI^{\pm}(\tau,\mu,\phi)}{d\tau} = I^{\pm}(\tau,\mu,\phi) - S^{\pm}(\tau,\mu,\phi).$$

The third term $S^{*\pm}(\tau,\mu,\phi)$ in Eq. 24 is:

- the solar "pseudo-source", which drives the diffuse radiation field in the case of collimated solar beam forcing.
- To describe this term we need to make a choice about how to treat the underlying surface as described below.

Surface Reflection, Transmission, and Emission (1)

We must know the reflectance, transmittance, and emittance of underlying surfaces to compute the diffuse radiation field.

It is frequently assumed that the underlying land or ocean surface reflects incoming radiation *isotropically*. Such a surface is called:

- a *Lambert* reflector, with reflectance, $\rho_{\rm L}$, the surface albedo.

Because most natural surfaces are *non*-Lambertian, we should use the bidirectional reflection distribution function (BRDF). Then:

- the radiative transfer problem that we have formulated is determined by solving Eq. 23 $[\pm\mu \frac{dI^{\pm}(\tau,\mu,\phi)}{d\tau} = I^{\pm}(\tau,\mu,\phi) - S^{\pm}(\tau,\mu,\phi)]$ with the pseudo-source:

$$S^{*\pm}_{\rm air}(\tau,\mu,\phi) = \frac{\varpi(\tau)\ F^s}{4\pi}\ p(\tau,-\mu_0,\phi_0;\pm\mu,\phi)\ e^{-\tau/\mu_0} \tag{27}$$

subject to the boundary condition at the TOA ($\tau = 0$):

$$I^{-}(0,\mu,\phi) = 0, \tag{28}$$

Surface Reflection, Transmission, and Emission (2)

and the boundary condition at bottom of the atmosphere ($\tau = \tau_{\rm a}$):

$$I^+(\tau_{\rm a}, \mu, \phi) = \int_0^{2\pi} d\phi' \int_0^1 d\mu' \mu' \rho_{\rm d}(-\mu', \phi'; +\mu, \phi) I^-(\tau_{\rm a}, \mu, \phi)$$

$$+ \frac{\mu_0}{\pi} \rho_{\rm d}(-\mu_0, \phi_0; +\mu, \phi) F^{\rm s} e^{-\tau_{\rm a}/\mu_0} + \epsilon(\mu) B(T_{\rm s}). \quad (29)$$

Here we have assumed that:

- the thermal emission, $\epsilon(\mu)$, is independent of ϕ, and $\rho_{\rm d}(-\mu', \phi'; +\mu, \phi)$ is the BRDF, which for a Lambert reflector reduces to $\rho_{\rm L}$.

For the *coupled atmosphere-ocean* system it is preferable to consider two strata:

- one for the atmosphere, and one for the ocean, but with *different indices of refraction*, $m_{\rm r}$.

Since the *basic radiance*, $I/m_{\rm r}^2$, is conserved (if no reflection):

- it must be constant across the interface between the two strata.
- *The basic radiance satisfies Snell's law and Fresnel's equation.*
- The downward radiation distributed over 2π sr in the atmosphere will be restricted to a cone less than 2π sr in the ocean.

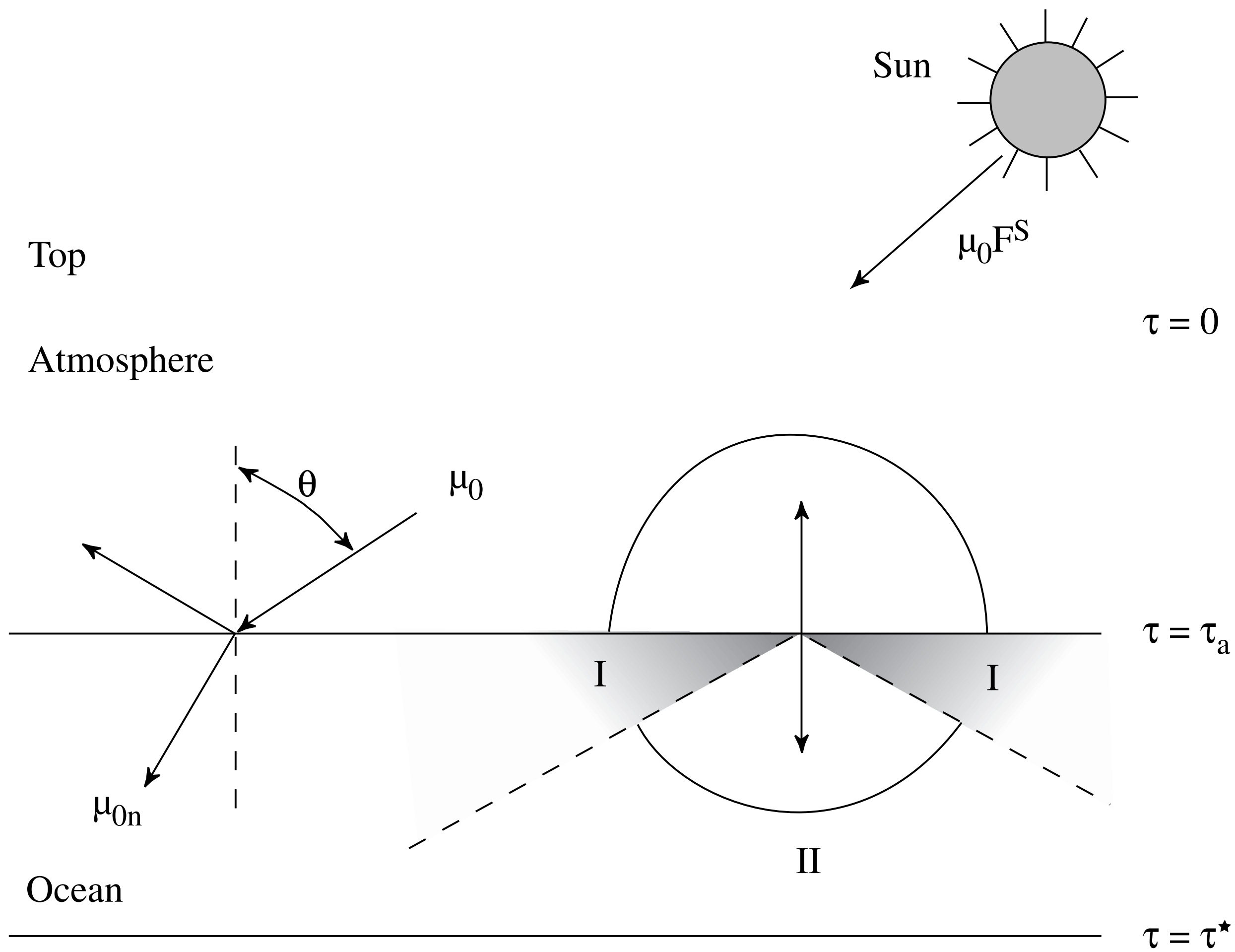

Figure 4: **Schematic illustration of two adjacent media with a flat interface such as the atmosphere overlying a calm ocean. Because the atmosphere has a different index of refraction ($m_\mathrm{r} \approx 1$) than the ocean ($m_\mathrm{r} \approx 1.34$), radiation distributed over 2π sr in the atmosphere will be confined to a cone less than 2π sr in the ocean (region II). Radiation in the ocean within region I will be totally reflected when striking the interface from below.**

Surface Reflection, Transmission, and Emission (4)

For a planar, smooth interface (a calm ocean), conservation of energy demands that (see Fig. 4):

Beams outside the refractive region in the ocean:

- are in the total reflection region (referred to as region I in Fig. 4).

The demarcation between the refractive and the total reflection region in the ocean is given by:

- the critical angle $\mu_c = \sqrt{1 - 1/m_{\text{rel}}^2}$, where $m_{\text{rel}} = m_{\text{r,ocn}}/m_{\text{r,air}}$ is the index of refraction of the ocean relative to the air.

For the atmosphere-ocean system, the source term $S^{*\pm}(\tau, \mu, \phi)$ in the air can be expressed as:

$$
\begin{aligned}
S_{\text{air}}^{*\pm}(\tau, \mu, \phi) &= \frac{\varpi(\tau) F^{\text{s}}}{4\pi} p(\tau, -\mu_0, \phi_0; \pm\mu, \phi)\, e^{-\tau/\mu_0} \\
&+ \frac{\varpi(\tau) F^{\text{s}}}{4\pi} p(\tau, \mu_0, \phi_0; \pm\mu, \phi)\, \mathcal{R}(-\mu_0, m_{\text{rel}})\, e^{-(2\tau_{\text{a}} - \tau)/\mu_0}. \quad (30)
\end{aligned}
$$

Surface Reflection, Transmission, and Emission (5)

Here $\tau_{\rm a}$ is the total optical depth of the atmosphere, $\mathcal{R}(-\mu_0, m_{\rm rel})$ is the Fresnel reflectance of the solar beam at the interface, and:

- the first term in Eq. 30 represents the contribution from the attenuated incident solar beam source, while
- the second term represents the contribution from the Fresnel reflection of this beam source by the air-water interface.

In the water, the source term can be written as:

$$S_{\rm w}^{*\pm}(\tau, \mu, \phi) = \frac{\varpi(\tau) F^{\rm s}}{4\pi} \frac{\mu_0}{\mu_{\rm t}} p(\tau, -\mu_t, \phi_0; \mu, \phi) e^{-\tau_{\rm a}/\mu_0} \mathcal{T}(-\mu_0, m_{\rm rel}) \, e^{-(\tau-\tau_{\rm a})/\mu_{\rm t}} \quad (31)$$

where $\mathcal{T}(-\mu_0, m_{\rm rel})$ is the transmittance through the air/water interface, $\mu_{\rm t}$ is the cosine of the SZA in the water (see Fig. 4), which is related to μ_0 by Snell's law:

$$\mu_{\rm t} = \sqrt{1 - (1 - \mu_0^2)/m_{\rm rel}^2} \quad (\rightarrow \ \mu_0 \quad \text{as} \quad m_{\rm rel} \rightarrow 1).$$

Surface Reflection, Transmission, and Emission (6)

In summary, the radiative transfer problem that we have formulated is determined by:

- solving Eq. 23 $[\pm\mu\frac{dI^{\pm}(\tau,\mu,\phi)}{d\tau} = I^{\pm}(\tau,\mu,\phi) - S^{\pm}(\tau,\mu,\phi)]$, with the pseudo-sources described by Eq. 30

  $[S^{*\pm}_{\rm air}(\tau,\mu,\phi) = \frac{\varpi(\tau)F^{\rm s}}{4\pi}\, p(\tau,-\mu_0,\phi_0;\pm\mu,\phi)\, e^{-\tau/\mu_0} + \frac{\varpi(\tau)F^{\rm s}}{4\pi}\, p(\tau,\mu_0,\phi_0;\pm\mu,\phi)\, \mathcal{R}(-\mu_0,m_{\rm rel})\, e^{-(2\tau_{\rm a}-\tau)/\mu_0}]$

  for the atmosphere, and Eq. 31

  $[S^{*\pm}_{\rm w}(\tau,\mu,\phi) = \frac{\varpi(\tau)F^{\rm s}}{4\pi}\frac{\mu_0}{\mu_{\rm t}}\, p(\tau,-\mu_{\rm t},\phi_0;\mu,\phi) e^{-\tau_{\rm a}/\mu_0}\, \mathcal{T}(-\mu_0,m_{\rm rel})\, e^{-(\tau-\tau_{\rm a})/\mu_{\rm t}}]$

  for the water, subject to:

- the boundary conditions given by Eq. 28 at $\tau = 0$, and by Eq. 29 with $\tau_{\rm a}$ replaced by τ^*, the total optical depth of the atmosphere-ocean system (see Fig. 4).

Note that:

- In mathematical terms the forward model that we have formulated corresponds to a *two-point boundary-value problem.*

Isolation of the Azimuthal Dependence (1)

To isolate the azimuth dependence in Eq. 23, we expand the scattering phase function $p(\tau, u', \phi'; u, \phi)$ in Legendre polynomials:

$$p(\tau, u', \phi'; u, \phi) \;=\; \sum_{m=0}^{2N-1} (2 - \delta_{0m})\, p^m(\tau, u', u) \cos m(\phi' - \phi) \tag{32}$$

where:

$$p^m(\tau, u', u) = \sum_{\ell=m}^{2N-1} (2\ell + 1)\chi_\ell(\tau)\Lambda_\ell^m(u')\Lambda_\ell^m(u). \tag{33}$$

Here $2N$ is the number of terms required to obtain an adequate representation of the scattering phase function, $\Lambda_\ell^m(u) \equiv \sqrt{(\ell - m)!/(\ell + m)!}\, P_\ell^m(u)$, $P_\ell^m(u)$ is the associated Legendre polynomial, and $\chi_\ell(\tau)$ is the expansion coefficient.

Expanding the radiance in a similar way:

$$I(\tau, u, \phi) = \sum_{m=0}^{2N-1} I^m(\tau, u)\ \cos m(\phi_0 - \phi) \tag{34}$$

one finds that each Fourier component satisfies the following radiative transfer equation (same as Eq. 23, except for ϕ-dependence):

Isolation of the Azimuthal Dependence (2)

$$\pm\mu\frac{dI^{m\pm}(\tau,\mu)}{d\tau} = I^{m\pm}(\tau,\mu) - S^{m\pm}(\tau,\mu) \qquad \text{where:} \tag{35}$$

$$S^{m\pm}(\tau,\mu) = \frac{\varpi(\tau)}{2}\int_{-1}^{1} du' p^m(\tau,u',\pm\mu)I^m(\tau,u') + S^{*m\pm}(\tau,\mu) + (1-\delta_{0m})S_{\rm TH}(\tau), \tag{36}$$

$p^m(\tau,u',\pm\mu)$ is given by Eq. 33, and

$$S^{*m\pm}(\tau,\mu) = X_0^m(\tau,\pm\mu)e^{-\tau/\mu_0} \tag{37}$$

$$X_0^m(\tau,\pm\mu) = \frac{\varpi(\tau)}{4\pi}F^{\rm s}(2-\delta_{0m})\sum_{\ell=m}^{2N-1}(-1)^{\ell+m}(2\ell+1)\chi_\ell(\tau)\Lambda_\ell^m(\pm\mu)\Lambda_\ell(\mu_0). \tag{38}$$

Since there is no diffuse radiation incident at the top of the atmosphere:

$$I^{m-}(\tau=0,\mu) = 0 \qquad \text{(see Eq. 28).} \tag{39}$$

At the lower boundary Eq. 29 applies with $\tau_{\rm a}$ replaced by τ^*:

$$\begin{aligned} I^+(\tau^*,\mu,\phi) \;&=\; \int_0^{2\pi} d\phi' \int_0^1 d\mu'\mu'\rho_{\rm d}(-\mu',\phi';+\mu,\phi)I^-(\tau^*,\mu,\phi) \\ &+\; \frac{\mu_0}{\pi}\rho_{\rm d}(-\mu_0,\phi_0;+\mu,\phi)F^{\rm s}e^{-\tau^*/\mu_0} + \epsilon(\mu)B(T_{\rm s}). \end{aligned} \tag{40}$$

To proceed we consider a multi-layered medium:

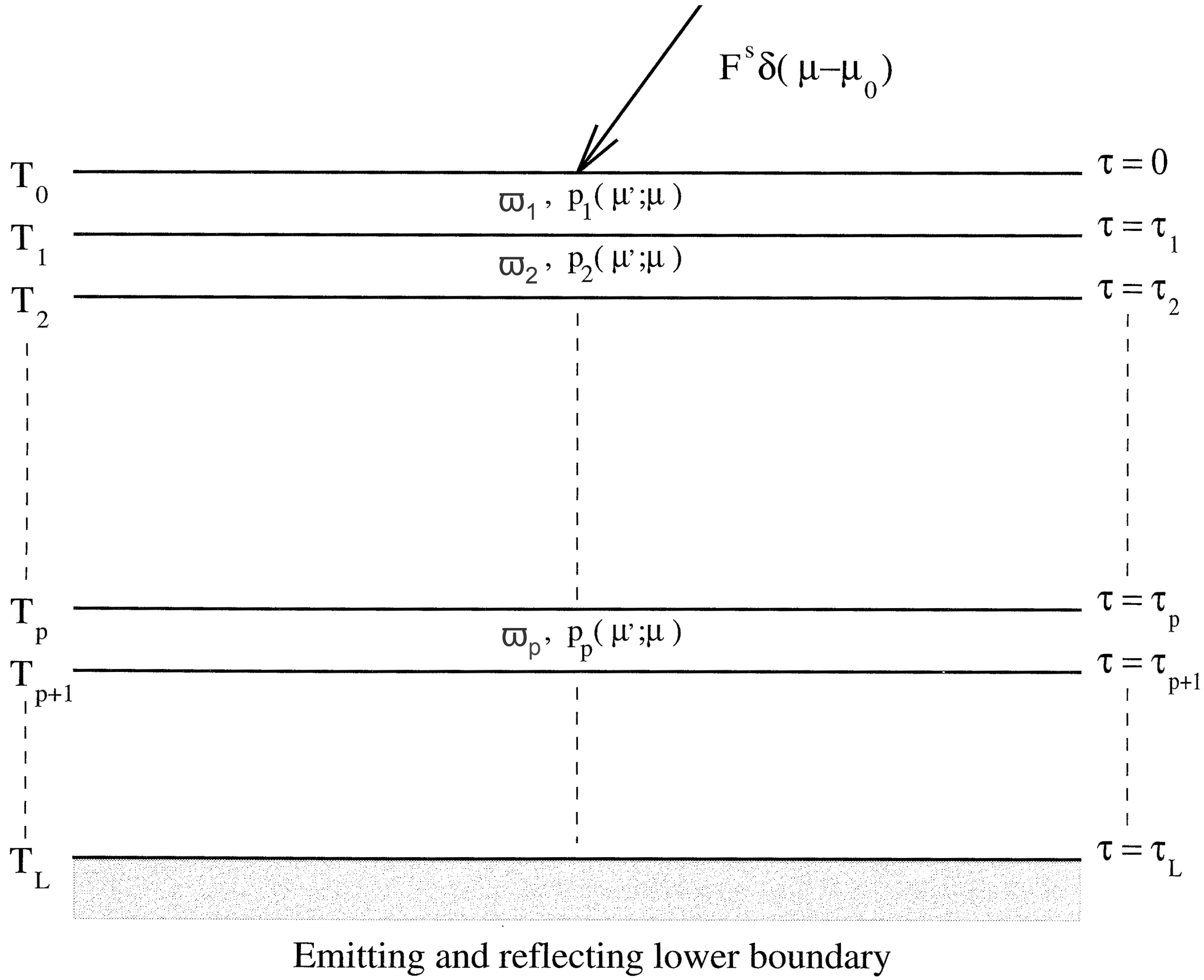

Figure 5: **Schematic illustration of a multi-layered, inhomogeneous medium overlying an emitting and partially reflecting surface.**

Discrete-Ordinate-Method – Brief Historical Perspective

The discrete-ordinate-method originated with:

- Wick and Chandrasekhar in the 1940's, and was
- extensively developed by Chandrasekhar as documented in his classic treatise: *Radiative Transfer*, 1950.

The method was almost abandoned due to numerical difficulties associated with:

- the computation of eigensolutions; and
- the computation of the constants of integration in a multi-layered medium.

However, the method has been rescued from oblivion:

- first by the work of Liou in the 1970's; and
- then by the work of Stamnes and co-workers in the 1980's.

The DISORT Radiative Transfer Method (1)

The set of equations formulated above may be solved by converting the *integro-differential* equations to:

- *a set of coupled ordinary differential* equations by replacing the integrals by quadrature sums. For a homogeneous slab:
- the discrete ordinate approximation to the radiative transfer equation (DISORT) is described by Stamnes et al. (1988; 2000).

Application of the discrete ordinate approximation to:

- $$\pm\mu \frac{dI^{m\pm}(\tau,\mu)}{d\tau} = I^{m\pm}(\tau,\mu) - S^{m\pm}(\tau,\mu) \qquad \text{(Eq. 35)}$$

  and Eq. 36

  $$S^{m\pm}(\tau,\mu) = \frac{\varpi(\tau)}{2}\int_{-1}^{1} du' p^m(\tau,u',\pm\mu) I^m(\tau,u') + S^{*m\pm}(\tau,\mu) + (1-\delta_{0m}) S_{\mathrm{TH}}(\tau)$$

  for a multi-layered air-water system with L_1 layers in the air, and L_2 in the water is described in some detail elsewhere [Jin and Stamnes, 1994; Stamnes, Thomas, and Stamnes, 2017].

The DISORT Radiative Transfer Method (2)

We approximate the integral over polar angles in Eq. 36 by a quadrature sum (numerical integration) consisting of:

- $2N_1$ terms or "streams" in the atmosphere: N_1 'streams' in the upper hemisphere and N_1 in the the downward hemisphere.

The N_1 'streams' in the downward hemisphere are refracted through the interface when the radiation penetrates into the water.

To represent the radiation in the total reflection region we need additional "streams." Thus, we choose:

- $2N_2$ $(N_2 > N_1)$ streams for the radiation in the water, implying:
- $2(N_2 - N_1)$ streams in the total reflection region.

The solution to the discrete ordinate approximation to Eqs. 35 and 36 for the radiance in discrete upward $(+\mu_i)$ and downward $(-\mu_i)$ directions in the p^{th} layer in the atmosphere becomes (dropping the m-superscript):

The DISORT Radiative Transfer Method (3)

$$I_p(\tau, \pm\mu_i^{\rm a}) = \sum_{j=1}^{N_1}[C_{-jp}g_{-jp}^{\rm a}(\pm\mu_i^{\rm a})e^{k_{jp}^{\rm a}\tau} + C_{jp}g_{jp}^{\rm a}(\pm\mu_i^{\rm a})e^{-k_{jp}^{\rm a}\tau}] + U_p(\tau, \pm\mu_i^{\rm a}) \quad (41)$$

where $i = 1, ..., N_1$ and $p \leq L_1$, and where the superscript "a" is used to denote atmospheric parameters.

Similary, for the p^{th} layer in the water, we have:

$$I_p(\tau, \pm\mu_i^{\rm w}) = \sum_{j=1}^{N_2}[C_{-jp}g_{-jp}^{\rm w}(\pm\mu_i^{\rm w})e^{k_{jp}^{\rm w}\tau} + C_{jp}g_{jp}^{\rm w}(\pm\mu_i^{\rm w})e^{-k_{jp}^{\rm w}\tau}] + U_p(\tau, \pm\mu_i^{\rm w}) \quad (42)$$

where $i = 1, ..., N_2$, $L_1 < p \leq L_1 + L_2$, and where the superscript "w" is used to denote aquatic parameters. Here:

- $k_{jp}^{\rm a}$, $g_{jp}^{\rm a}$, $k_{jp}^{\rm w}$, and $g_{jp}^{\rm w}$ are eigenvalues and eigenvectors required for the homogeneous solution to Eq. 35 [$S^{*\pm}(\tau, \mu) = S_{\rm TH}(\tau) = 0$ in Eq. 36; ignoring the m-superscript].
- The term $U_p(\tau, \pm\mu)$ represents the particular solution.

The DISORT Radiative Transfer Method (4)

The coefficients $C_{\pm jp}$ are determined by applying:

- (i) boundary conditions at the top of the atmosphere and the bottom of the water,
- (ii) radiance continuity conditions at each interface between the layers, and
- (iii) Fresnel's equations at the atmosphere-water interface as discussed above [see Stamnes, Thomas, and Stamnes, 2017 for details].

This procedure leads to a system of linear algebraic equations of the form:

$$\mathbf{A}\mathbf{x} = \mathbf{B} \tag{43}$$

which has solution

$$\mathbf{x} = \mathbf{A}^{-1}\mathbf{B}.$$

The DISORT Radiative Transfer Method (5)

The matrix $\mathbf{A}$ contains information about:

- the system inherent optical properties (layer-by-layer) as well as the lower boundary BRDF properties.

The column vector $\mathbf{x}$ contains:

- all the unknown coeffcients, the $C_{\pm jp}$, and

the column vector $\mathbf{B}$ contains:

- information about the particular solutions as well as the lower boundary emissivity.

The dimension of the matrix $\mathbf{A}$ is:

- $(2N_1 \times L_1) + (2N_2 \times L_2)$, the same as the number of unknown coefficients $C_{\pm jp}$.

The DISORT Radiative Transfer Method (6)

To compute the diffuse radiance and the corresponding irradiances we need to turn the formalism outlined above into a suitable radiative transfer code:

- For a single slab with a constant index of refraction the DISORT code [Stamnes et al., 1988, 2000; Lin et al., 2015 (DISORT3)] is available.

This code was extended by Jin and Stamnes (1994) to:

- apply to the coupled atmosphere-ocean (CAO) system as described above to allow for radiances to be computed at the quadrature angles at any desired level in the atmosphere-ocean system.

The method was extended (Yan and Stamnes, 2002):

- to compute radiances at arbitrary angles (not just the discrete quadrature angles) by integrating the source function as indicated schematically in Eq. 7:

$$
\begin{aligned}
I[\nu, \tau(s_2), \hat{\Omega}] &= \\
&= I[\nu, \tau(s_1), \hat{\Omega}] e^{-[\tau(s_2) - \tau(s_1)]} + \int_{\tau(s_1)}^{\tau(s_2)} dt S(\nu, t(s), \hat{\Omega}) e^{-[\tau(s_2) - t(s)]}
\end{aligned}
$$

The DISORT Radiative Transfer Method (7)

In summary the CAO-DISORT method works as follows:

1. The air and water are treated as two adjacent plane-parallel media (slabs) separated by an interface across which the index of refraction changes from $m_{\rm r} \approx 1.0$ in air to $m_{\rm r} \approx 1.34$ in water.
2. Each of the two slabs is divided into a sufficient number of layers to adequately resolve the variation of the IOPs.
3. The reflection by and transmission through the air-water interface are computed by Fresnel's equations, and the bending of the rays across the interface follows Snell's law.
4. The radiative transfer equation is solved separately for each layer in the atmosphere and water using the discrete-ordinate method.
5. The solution is completed by applying boundary conditions at the TOA and bottom of the water as well as radiance continuity conditions at layer interfaces in the atmosphere as well in the water.

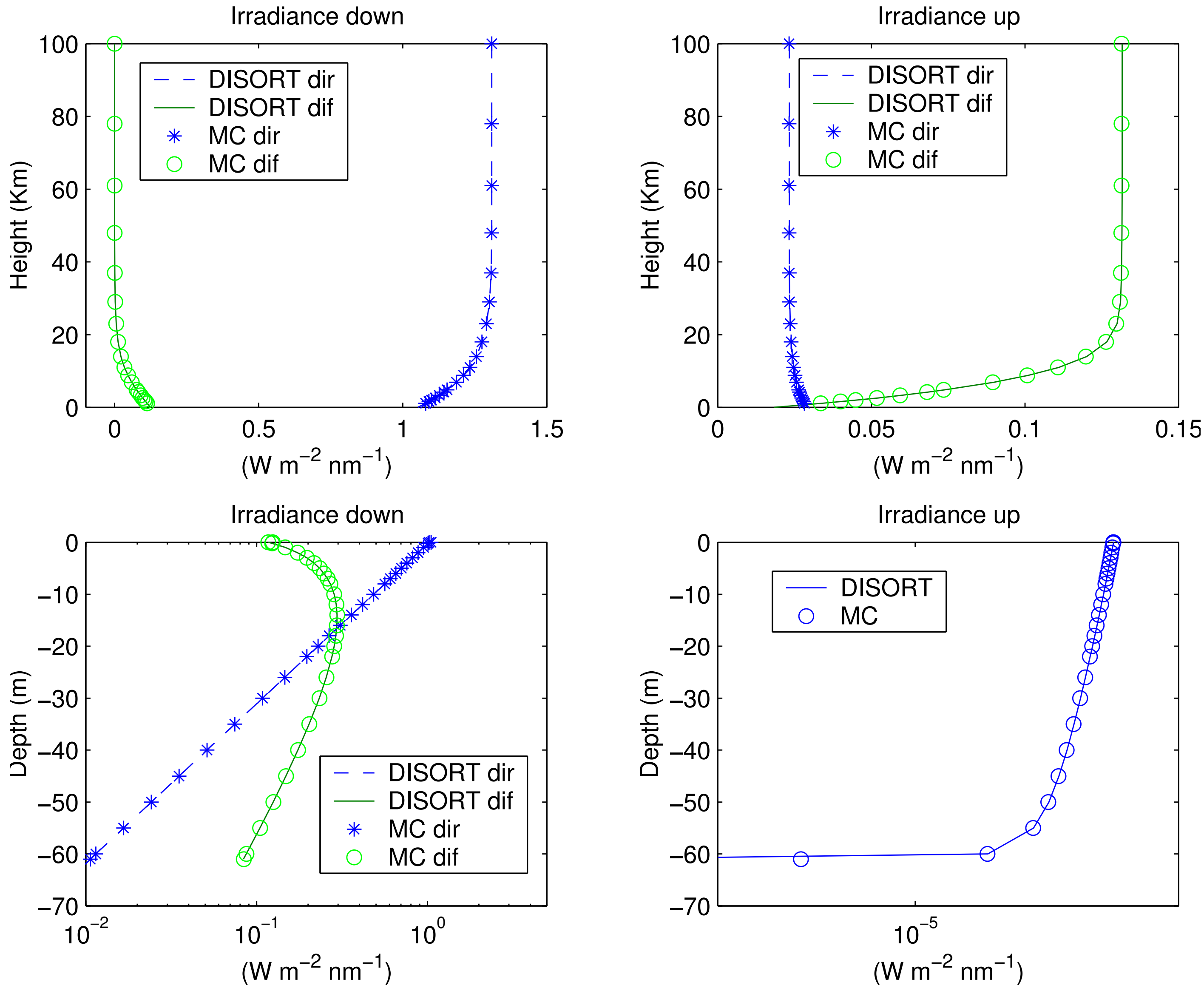

Figure 6: **Comparison of CAO-DISORT and Monte Carlo Results for the Coupled Atmopshere Ocean System (Gjerstad et al., 2003).**

The Discrete-Ordinate Method: Mathematical and Numerical Aspects

- Formulation and Overview – Brief Review
- **Discrete Ordinate Method – Isotropic Scattering – Quadrature Formulas**
- Discrete Ordinate Method – Anisotropic Scattering
- Matrix Formulation of the Discrete Ordinate Method
- Matrix Eigensolutions
- Solutions to Prototype Problems
- Boundary Conditions – Removal of Ill-Conditioning
- Multi-Layered Inhomogeneous Slab
- **Source Functions and Angular Distributions**
- Computational Example

Overview – (1)

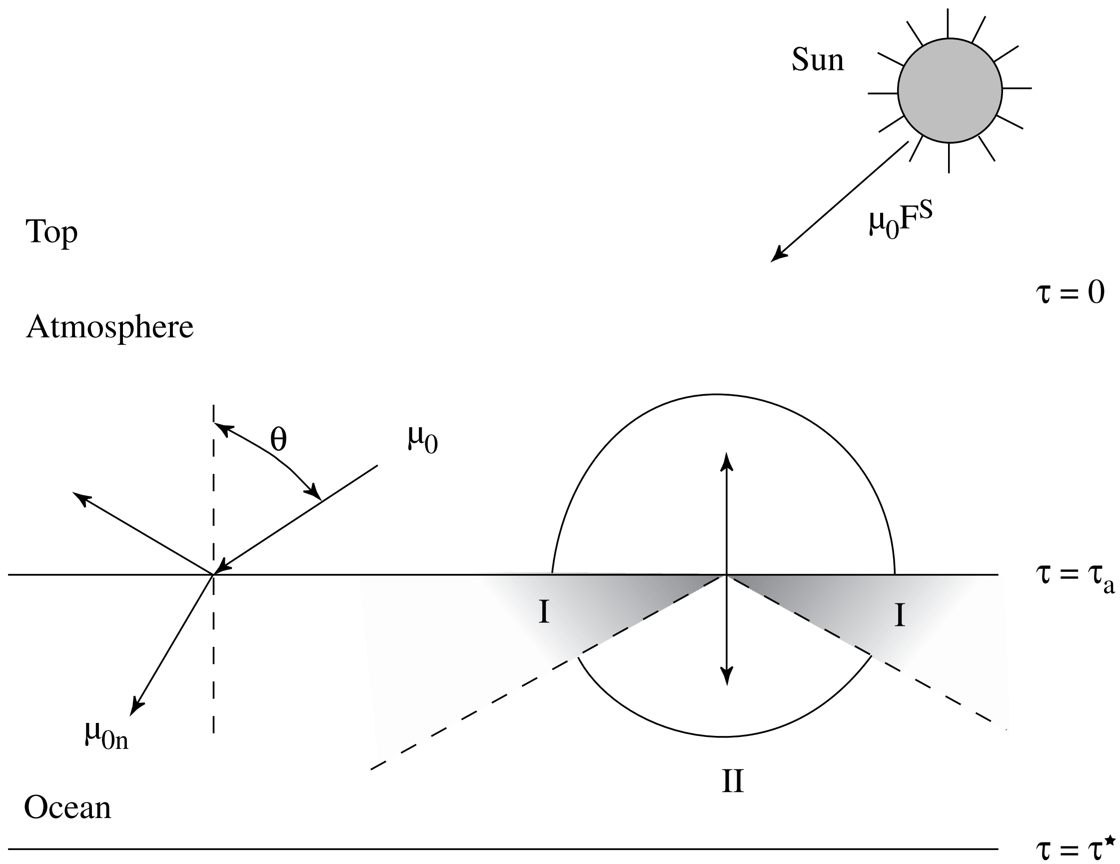

Figure 7: **Schematic illustration of two adjacent media with a flat interface such as the atmosphere overlying a calm ocean. Because the atmosphere has a different index of refraction ($m_r \approx 1$) than the ocean ($m_r \approx 1.34$), radiation distributed over 2π sr in the atmosphere will be confined to a cone less than 2π sr in the ocean (region II). Radiation in the ocean within region I will be totally reflected when striking the interface from below.**

Overview – (2)

The RT problem we formulated involves solving:

$$\pm\mu \frac{dI^{\pm}(\tau,\mu,\phi)}{d\tau} = I^{\pm}(\tau,\mu,\phi) - S^{\pm}(\tau,\mu,\phi)$$

where $S^{\pm}(\tau,\mu,\phi) = S_{\rm TH}(\tau) + S^{\pm}_{\rm MS}(\tau,\mu,\phi) + S^{*\pm}(\tau,\mu,\phi)$ with thermal contribution $S_{\rm TH}(\tau) = [1-\varpi(\tau)]B[T(\tau)]$, multiple scattering contribution

$$S^{\pm}_{\rm MS}(\tau,\mu,\phi) = \frac{\varpi(\tau)}{4\pi} \int_0^{2\pi} d\phi' \int_{-1}^{1} du' \, p(\tau,u',\phi';\pm\mu,\phi) I(\tau,u',\phi')$$

and pseudo-sources described by

$$S^{*\pm}_{\rm air}(\tau,\mu,\phi) = \frac{\varpi(\tau)F^s}{4\pi} p(\tau,-\mu_0,\phi_0;\pm\mu,\phi)\, e^{-\tau/\mu_0} + \frac{\varpi(\tau)F^s}{4\pi} p(\tau,\mu_0,\phi_0;\pm\mu,\phi)\, \mathcal{R}(-\mu_0,m_{\rm rel})\, e^{-(2\tau_{\rm a}-\tau)/\mu_0}$$

in the atmosphere, and (τ^* = total optical depth of atmosphere–ocean system)

$$S^{*\pm}_{\rm w}(\tau,\mu,\phi) = \frac{\varpi(\tau)F^{\rm s}}{4\pi}\frac{\mu_0}{\mu_{\rm t}} p(\tau,-\mu_{\rm t},\phi_0;\mu,\phi) e^{-\tau_{\rm a}/\mu_0}\, \mathcal{T}(-\mu_0,m_{\rm rel})\, e^{-(\tau-\tau_{\rm a})/\mu_{\rm t}}$$

in the water, subject to: boundary condition: $I^{-}(0,\mu,\phi) = 0$ at TOA, and

$$I^{+}(\tau^*,\mu,\phi) = \int_0^{2\pi} d\phi' \int_0^1 d\mu' \mu' \rho_{\rm d}(-\mu',\phi';+\mu,\phi) I^{-}(\tau^*,\mu',\phi') + \epsilon(\mu)B(T_{\rm s})$$

$$+ \frac{\mu_0}{\pi}\rho_{\rm d}(-\mu_0,\phi_0;+\mu,\phi)\frac{\mu_0}{\mu_{\rm t}}\mathcal{T}(-\mu_0,m_{\rm rel})F^{\rm s}\, e^{-\tau_{\rm a}/\mu_0} e^{-(\tau^*-\tau_{\rm a})/\mu_{\rm t}}. \quad (44)$$

Overview – (3)

To isolate the azimuth dependence in RTE: expand phase function:

$$p(\tau, u', \phi'; u, \phi) \; = \; \sum_{m=0}^{2N-1} (2 - \delta_{0m}) \, p^m(\tau, u', u) \cos m(\phi' - \phi) \tag{45}$$

$$p^m(\tau, u', u) = \sum_{\ell=m}^{2N-1} (2\ell + 1)\chi_\ell(\tau)\Lambda_\ell^m(u')\Lambda_\ell^m(u). \tag{46}$$

Here $2N$ = # of terms required to obtain an adequate representation of the phase function, $\Lambda_\ell^m(u) \equiv \sqrt{(\ell - m)!/(\ell + m)!} \, P_\ell^m(u)$, $P_\ell^m(u)$ = associated Legendre polynomial, and $\chi_\ell(\tau)$ = expansion coefficient. Expanding the radiance similarly:

$$I(\tau, u, \phi) = \sum_{m=0}^{2N-1} I^m(\tau, u) \; \cos \; m(\phi_0 - \phi) \tag{47}$$

one finds that each Fourier component satisfies the following RTE:

$$\pm\mu \frac{dI^{m\pm}(\tau, \mu)}{d\tau} = I^{m\pm}(\tau, \mu) - S^{m\pm}(\tau, \mu) \tag{48}$$

$$S^{m\pm}(\tau, \mu) = \frac{\varpi(\tau)}{2} \int_{-1}^{1} du' p^m(\tau, u', \pm\mu) I^m(\tau, u') + S^{*m\pm}(\tau, \mu) + (1 - \delta_{0m}) S_{\mathrm{TH}}(\tau) \tag{49}$$

and $p^m(\tau, u', \pm\mu)$ is given by Eq. 33, and

$$S^{*m\pm}(\tau, \mu) = X_0^m(\tau, \pm\mu) e^{-\tau/\mu_0} \tag{50}$$

$$X_0^m(\tau, \pm\mu) = \frac{\varpi(\tau)}{4\pi} F^{\mathrm{s}} (2 - \delta_{0m}) \sum_{\ell=m}^{2N-1} (-1)^{\ell+m} (2\ell + 1)\chi_\ell(\tau)\Lambda_\ell^m(\pm\mu)\Lambda_\ell^m(\mu_0) \tag{51}$$

RTE equations

Now recall that substitution of

$$p(\tau,u',\phi';u,\phi) \;=\; \sum_{m=0}^{2N-1}(2-\delta_{0m})p^m(\tau,u',u)\cos m(\phi'-\phi)$$

$p^m(\tau,u',u)=\sum_{\ell=m}^{2N-1}(2\ell+1)\chi_\ell\Lambda_\ell^m(u')\Lambda_\ell^m(u)$, $\quad \Lambda_\ell^m(u)\equiv\sqrt{\frac{(\ell-m)!}{(\ell+m)!}}\,P_\ell^m(u)$ and:

$$I(\tau,u,\phi)=\sum_{m=0}^{2N-1}I^m(\tau,u)\cos m(\phi_0-\phi)$$

into the full-range slab geometry RTE:

$$u\frac{dI(\tau,u,\phi)}{d\tau} \;=\; I(\tau,u,\phi)-\frac{\varpi(\tau)}{4\pi}\int_0^{2\pi}d\phi'\int_{-1}^{1}du'p(\tau,u',\phi';u,\phi)I(\tau,u',\phi')-(1-\varpi(\tau))B-S^*(\tau,u,\phi) \quad (52)$$

yields:

$$\begin{aligned} u\frac{dI^m(\tau,u)}{d\tau} \;&=\; I^m(\tau,u)-\frac{\varpi(\tau)}{2}\int_{-1}^{1}du'p^m(\tau,u',u)I^m(\tau,u')-X_0^m(\tau,u)e^{-\tau/\mu_0} \\ &\quad -(1-\varpi(\tau))B(\tau)\delta_{0m} \qquad\qquad (m=0,1,2,\ldots,2N-1). \end{aligned} \quad (53)$$

$$X_0^m(\tau,u)=\frac{\varpi(\tau)}{4\pi}F^s(2-\delta_{0m})\sum_{\ell=m}^{2N-1}(-1)^{\ell+m}(2\ell+1)\chi_\ell(\tau)\Lambda_\ell^m(u)\Lambda_\ell^m(\mu_0). \quad (54)$$

Accurate Numerical Solutions (1)

Accurate techniques include:

- The **discrete-ordinate method** $\longrightarrow$ **two-stream approximation**;
- The **spherical-harmonic method** $\longrightarrow$ **Eddington approximation**;
- The **doubling-adding method**.

In "in lowest order" the first two methods become the **two-stream**, and **Eddington approximations**, respectively.

Discrete-Ordinate Method – Isotropic Scattering

Quadrature Formulas

- The solution of the isotropic-scattering problem involves the following integral over angle ($p^m(\tau, u', u) = 1$):

$$\int_{-1}^{1} du\, I(\tau, u) = \int_0^1 d\mu\, I^+(\tau, \mu) + \int_0^1 d\mu\, I^-(\tau, \mu).$$

Accurate Numerical Solutions (2)

- In the two-stream method:

$$\int_{-1}^{1} du\ I \approx I^{+}(\tau) + I^{-}(\tau).$$

- We could improve the accuracy by including more points:

$$\int_{-1}^{1} du\ I(\tau, u) \approx \sum_{j=1}^{m} w'_j I(\tau, u_j) \quad \text{where}$$

- w'_j is a **quadrature weight** and u_j is the **discrete ordinate**.
- The simplest example is the **trapezoidal rule**:

$$\int_{-1}^{1} du\ I \approx \Delta u(\frac{1}{2}I_1 + I_2 + I_3 + \cdots + I_{m-1} + \frac{1}{2}I_m)$$

- The more accurate Simpson's rule is:

$$\int_{-1}^{1} duI \approx \frac{\Delta u}{3}(I_1 + 4I_2 + 2I_3 + 4I_4 + \cdots + I_m)$$

where

- Δu is the (equal) spacing between the adjacent points, u_j, and the $I_j \equiv I(\tau, u_j)$.

Accurate Numerical Solutions (3)

INTERPOLATION FORMULA

- If we have m points at which we evaluate $I(\tau, u)$, we can replace $I(\tau, u)$ with its **approximating polynomial** $\phi(u)$, which is a polynomial of degree $(m-1)$.
- Consider the following form for $\phi(u)$, for $m = 3$:

$$\begin{aligned}\phi(u) \;&=\; I(u_1)\frac{(u-u_2)(u-u_3)}{(u_1-u_2)(u_1-u_3)} + I(u_2)\frac{(u-u_1)(u-u_3)}{(u_2-u_1)(u_2-u_3)} \\ &\quad + I(u_3)\frac{(u-u_1)(u-u_2)}{(u_3-u_1)(u_3-u_2)}.\end{aligned}$$

- $\phi(u)$ is a second-degree polynomial which, when evaluated at the points u_1, u_2, and u_3, yields $\phi(u_1) = I(u_1)$, $\phi(u_2) = I(u_2)$, and $\phi(u_3) = I(u_3)$, respectively.
- $\phi(u)$ is an example of **Lagrange's interpolation formula, which we can write as follows. First, we define:**

$$F(u) \equiv \prod_{j=1}^{m}(u-u_j) = (u-u_1)(u-u_2)\cdots(u-u_m).$$

Accurate Numerical Solutions (4)

- Then, since $(u-u_1)(u-u_2)\cdots(u-u_{j-1})(u-u_{j+1})\cdots(u-u_m)$ becomes:

$$F(u)/(u-u_j) = \prod_{k\neq j}^{m}(u-u_k)$$

we can write the polynomial $\phi(u)$ in a shorthand form:

$$\phi(u) = \sum_{j=1}^{m} I(u_j)\frac{F(u)}{(u-u_j)F'(u_j)} \qquad F'(u_j) \equiv dF/du\rfloor_{u=u_j}.$$

- The derivative will give a long string of polynomials of degree $(m-1)$; however, when it is evaluated at $u=u_j$, all terms vanish except the term $(u-u_1)(u-u_2)\cdots(u-u_{j-1})(u-u_{j+1})\cdots(u-u_m)$.

- Hence, the quadrature formula arising from the assumption that the radiance is a polynomial of degree $(m-1)$ is:

$$\int_{-1}^{1} du\, I(u) = \sum_{j=1}^{m} w'_j I(u_j); \qquad w'_j = \frac{1}{F'(u_j)}\int_{-1}^{1}\frac{du\, F(u)}{(u-u_j)}.$$

The quadrature points u_j are, so far, arbitrary.

Accurate Numerical Solutions (5)

- **The error incurred by using the Lagrange interpolation formula is proportional to the m^{th} derivative of the functions $[I(u)]$ being approximated.*[*]**
- Thus, it is clear that *if* $I(\tau, u)$ happens to be a polynomial of degree $(m-1)$ or smaller, then the m-point quadrature formula is exact. **We may now ask:**
- **Is it possible to obtain higher accuracy?** For example, by choosing the quadrature points in an optimal manner? **Gauss showed that:**
- If $F(u)$ is a certain polynomial, and the u_j are the roots of that polynomial, then we get the accuracy of a polynomial of degree $(2m-1)$.
- This polynomial is the **Legendre polynomial** $P_m(u)$. It has the special property of being orthogonal to every power of u less than m, i.e.:

$$\int_{-1}^{1} du\, P_m(u) u^l = 0 \qquad (l = 0, 1, 2, \cdots, m-1).$$

- Note that if u_j is a root of an even Legendre polynomial, then $-u_j$ is also a root. Also, all m roots are real.

[*]See, e. g., Burden, R. L., and J. D. Faires, *Numerical Analysis*, Prindle, Weber and Schmidt, Third Edition, Boston, 1985, p. 153.

Accurate Numerical Solutions (6)

The Double-Gauss Method

- It is customary to choose the **even-order** Legendre polynomials as the approximating polynomial. This choice is made because:
- The roots of the even-orders appear in **pairs**: $u_{-i} = -u_{+i}$.
- The quadrature weights are the same in each hemisphere, i.e., $w'_i = w'_{-i}$.
- The 'full-range' approach assumes that $I(\tau, u)$ is a smoothly-varying function of u $(-1 \leq u \leq +1)$ with no "sharp corners" for all values of τ.
- For small τ, the intensity changes rather rapidly as u passes through zero. In fact, at $\tau = 0$, this change is quite abrupt:
- $I(\tau = 0, u) = 0$ for slightly negative u-values; for slightly positive u-values it will generally have a finite value.
- It is difficult to 'fit' such a discontinuous distribution with a low-order polynomial that span the full range between $u = -1$ and $u = 1$.
- It is most difficult to get accurate solutions near the surface $(\tau = 0)$:
- **we should pay the most attention to this region.**

Accurate Numerical Solutions (7)

To remedy this situation, the **'Double-Gauss' method** was devised:

- We break the angular integration into two hemispheres, and approximate each integral separately:

$$\int_{-1}^{1} du\, I = \int_0^1 d\mu\, I^+ + \int_0^1 d\mu\, I^- \approx \sum_{j=1}^{M} w_j I^+(\mu_j) + \sum_{j=1}^{M} w_j I^-(\mu_j).$$

- The w_j and μ_j are the weights and roots of the approximating polynomial for the half-range. Note: we use the **same** set of w_j and μ_j for both hemispheres.
- To obtain the highest accuracy, we must again use **Gaussian quadrature.** However, our new interval is $(0 \leq \mu \leq 1)$ instead of $(-1 \leq u \leq 1)$.
- This new interval $(0 \leq \mu \leq 1)$ is easily arranged by defining the variable $u = 2\mu - 1$, so that the orthogonal polynomial is $P_M(2\mu - 1)$.

The new quadrature weight is given by:

$$w_j = \frac{1}{P'_M(2\mu_j - 1)} \int_0^1 d\mu \frac{P_M(2\mu - 1)}{(\mu - \mu_j)} \tag{55}$$

and the μ_j are the roots of the half-range polynomials.

Accurate Numerical Solutions (8)

- Algorithms to compute the roots and weights are usually based on the full range:
- Must relate the half-range quadrature μ_j and w_j to u_j and w'_j for the full range.
- Since the linear transformation $t = (2x - x_1 - x_2)/(x_2 - x_1)$ maps any interval $[x_1, x_2]$ into $[-1, 1]$ provided $x_2 > x_1$, Gaussian quadrature (GQ) yields:

$$\int_{x_1}^{x_2} dx I(x) = \int_{-1}^{1} dt I\left(\frac{(x_2 - x_1)t + x_2 + x_1}{2}\right) \frac{x_2 - x_1}{2}.$$

Choosing $x_1 = 0$, $x_2 = 1$, $x = \mu$ and $t = u$, we find:

$$\int_0^1 d\mu I(\mu) = \frac{1}{2}\int_{-1}^{1} du I\left(\frac{u+1}{2}\right)$$

and applying GQ to each integral, we find on setting $M = 2N$ for the half-range:

$$\int_0^1 d\mu I(\mu) = \sum_{j=1}^{2N} w_j I(\mu_j) = \frac{1}{2}\int_{-1}^{1} du I\left(\frac{u+1}{2}\right) = \frac{1}{2}\sum_{\substack{j=-N \\ j\neq 0}}^{N} w'_j I\left(\frac{u_j+1}{2}\right). \tag{56}$$

- Thus, in even orders:

$$\mu_j = \frac{u_j + 1}{2}; \qquad w_j = \frac{1}{2}w'_j. \tag{57}$$

Accurate Numerical Solutions (9)

Anisotropic Scattering

- We will generalize the **discrete ordinate method** to anisotropic scattering in finite inhomogeneous (layered) media.

We introduce a matrix formulation, because:

- it allows for a compact notation and facilitates the numerical implementation;
- it is valid for isotropic scattering as well as for any scattering phase function.

For simplicity we start by considering a homogeneous slab.

- Recall: When the radiance is written as a Fourier cosine series, each Fourier component satisfies a RTE mathematically identical to the azimuthally-averaged equation.
- Thus, we may focus on the RTE for the $m = 0$ component (or the scaled version if we want to utilize the δ-M scaling):

$$u\frac{dI(\tau,u)}{d\tau} = I(\tau,u) - \frac{\varpi(\tau)}{2}\int_{-1}^{1} du' p(\tau,u',u) I(\tau,u') - X_0(\tau,u)e^{-\tau/\mu_0}. \qquad (58)$$

Accurate Numerical Solutions (10)

- Mathematically, un-scaled and scaled equations are identical: scaling influences the optical properties of the medium, but will not affect the mathematics.
- Therefore, consider the following pair of coupled equations for half-range diffuse radiances, $I^m(\tau, \mu)$ with $m = 0$ (similar equations for $m \neq 0$):

$$\mu \frac{dI^+(\tau,\mu)}{d\tau} = I^+(\tau,\mu) - \frac{\varpi}{2}\int_0^1 d\mu'\, p(\mu',\mu) I^+(\tau,\mu') - \frac{\varpi}{2}\int_0^1 d\mu'\, p(-\mu',\mu) I^-(\tau,\mu') - X_0^+ e^{-\tau/\mu_0} \tag{59}$$

$$-\mu \frac{dI^-(\tau,\mu)}{d\tau} = I^-(\tau,\mu) - \frac{\varpi}{2}\int_0^1 d\mu'\, p(\mu',-\mu) I^+(\tau,\mu') - \frac{\varpi}{2}\int_0^1 d\mu'\, p(-\mu',-\mu) I^-(\tau,\mu') - X_0^- e^{-\tau/\mu_0} \tag{60}$$

where

$$p(\mu',\mu) = \sum_{\ell=0}^{2N-1} (2\ell+1)\chi_\ell P_\ell(\mu) P_\ell(\mu') \tag{61}$$

$$X_0^\pm \equiv X_0(\pm\mu) = \frac{\varpi}{4\pi} F^{\mathrm{s}} p(-\mu_0, \pm\mu). \tag{62}$$

Accurate Numerical Solutions (11)

We consider the collimated beam case for which we need to deal with the:

- full azimuthal dependence: $I(\tau, u, \phi) = \sum_{m=0}^{2N-1} I^m(\tau, u) \cos m(\phi_0 - \phi)$.

The discrete ordinate approximation to the half-range RTE is obtained by:

- For each m, replacing the integrals by sums to transform the pair of coupled integro-differential equations into a system of coupled $2N$ ODEs ($i = 1, \ldots N$):

$$\mu_i \frac{dI^+(\tau, \mu_i)}{d\tau} = I^+(\tau, \mu_i) - \frac{\varpi}{2} \sum_{j=1}^{N} w_j p(\mu_j, \mu_i) I^+(\tau, \mu_j) - \frac{\varpi}{2} \sum_{j=1}^{N} w_j p(-\mu_j, \mu_i) I^-(\tau, \mu_j) - X_{0i}^+ e^{-\tau/\mu_0} \tag{63}$$

$$-\mu_i \frac{dI^-(\tau, \mu_i)}{d\tau} = I^-(\tau, \mu_i) - \frac{\varpi}{2} \sum_{j=1}^{N} w_j p(\mu_j, -\mu_i) I^+(\tau, \mu_j) - \frac{\varpi}{2} \sum_{j=1}^{N} w_j p(-\mu_j, -\mu_i) I^-(\tau, \mu_j) - X_{0i}^- e^{-\tau/\mu_0}. \tag{64}$$

- We use the same quadrature in each hemisphere: $\mu_{-i} = -\mu_i$ and $w_{-i} = w_i$.

Accurate Numerical Solutions (12)

- Gaussian quadrature ensures that the phase function is correctly normalized:

$$\sum_{\substack{j=-N \\ j\neq 0}}^{N} w_j p(\tau, \mu_i, \mu_j) = \sum_{\substack{i=-N \\ i\neq 0}}^{N} w_i p(\tau, \mu_i, \mu_j) = 1. \tag{65}$$

Advantages of Expanding the the Phase Function in Legendre Polynomials are:

- (i) **Normalization holds for arbitrary values of** N;
  (ii) the "isolation" of the azimuth dependence is accomplished.

The Main Advantage of the "Double-Gauss" Scheme is that:

- The quadrature points (in even orders) are distributed symmetrically around $|u| = 0.5$ and clustered both towards $|u| = 1$ and $|u| = 0$, WHEREAS
- In full-range $(-1 < u < 1)$ Gaussian scheme, they are clustered towards $u = \pm 1$.
- The clustering towards $|u| = 0$ will give superior results near the boundaries where the intensity varies rapidly around $|u| = 0$.
- A half-range scheme is also preferable since the intensity is discontinuous at the boundaries.

Accurate Numerical Solutions (13)

- Another advantage is that half-range quantities such as $F^{\pm}$ and $\bar{I}^{\pm}$ are obtained immediately without any further approximations.

Matrix Formulation of the Discrete-Ordinate Method

- Before we consider the general multi-stream solution, we shall first describe the two-and four-stream cases ($N = 1$ and 2).

Two-stream approximation ($N = 1$):

The two-stream approximation is obtained by:

- Setting $N = 1$ in the half-range RTE (Eqs. 63 and 64) yields 2 coupled ODEs:

$$\mu_1 \frac{dI^+(\tau)}{d\tau} = I^+(\tau) - \frac{\varpi}{2} p(-\mu_1, \mu_1) I^-(\tau) - \frac{\varpi}{2} p(\mu_1, \mu_1) I^+(\tau) - Q'^+(\tau) \quad (66)$$

$$-\mu_1 \frac{dI^-(\tau)}{d\tau} = I^-(\tau) - \frac{\varpi}{2} p(-\mu_1, -\mu_1) I^-(\tau) - \frac{\varpi}{2} p(\mu_1, -\mu_1) I^+(\tau) - Q'^-(\tau) \quad (67)$$

where

Accurate Numerical Solutions (14)

$$
\begin{aligned}
I^{\pm}(\tau) &\equiv I^{\pm}(\tau,\mu_1) \\
Q'^{\pm}(\tau) &\equiv \frac{\varpi}{4\pi} F^{\mathrm{s}} p(-\mu_0, \pm\mu_1) e^{-\tau/\mu_0} \\
\frac{\varpi}{2} p(\mu_1, -\mu_1) &\equiv \frac{\varpi}{2}(1 - 3g\mu_1^2) \equiv \varpi b = \frac{\varpi}{2} p(-\mu_1, \mu_1) \\
\frac{\varpi}{2} p(\mu_1, \mu_1) &\equiv \frac{\varpi}{2}(1 + 3g\mu_1^2) \equiv \varpi(1 - b) = \frac{\varpi}{2} p(-\mu_1, -\mu_1).
\end{aligned}
$$

Recall that:

- $b \equiv \frac{1}{2}(1 - 3g\mu_1^2)$ is called the backscattering ratio and that g is the first moment of the scattering phase function, commonly referred to as the asymmetry factor.
- If we take $\mu_1 = 1/\sqrt{3}$, then $b = \frac{1}{2}(1 - g) \Longrightarrow$
  - for $g = -1$ we have complete backscattering ($b = 1$),
  - for $g = 1$ complete forward scattering ($b = 0$), and
  - for $g = 0$ isotropic scattering ($b = \frac{1}{2}$).
- The value $\mu_1 = 1/\sqrt{3}$ corresponds to Gaussian quadrature for the full-range $[-1, 1]$, while Gaussian quadrature for the half range $[0, 1]$ (referred to as Double-Gauss) yields $\mu_1 = \frac{1}{2}$.

Accurate Numerical Solutions (15)

We may rewrite Eqs. 66 and 67 in matrix form as:

$$\frac{d}{d\tau}\begin{bmatrix} I^+ \\ I^- \end{bmatrix} = \begin{bmatrix} -\alpha & -\beta \\ \beta & \alpha \end{bmatrix}\begin{bmatrix} I^+ \\ I^- \end{bmatrix} - \begin{bmatrix} Q^+ \\ Q^- \end{bmatrix} \tag{68}$$

where

$$Q^{\pm} \equiv \pm\mu_1^{-1}Q'^{\pm}$$

$$\alpha \equiv \left[\frac{\varpi}{2}p(\mu_1,\mu_1) - 1\right]/\mu_1 = \left[\frac{\varpi}{2}p(-\mu_1,-\mu_1) - 1\right]/\mu_1 = [\varpi(1-b) - 1]/\mu_1$$

$$\beta \equiv \frac{\varpi}{2}p(\mu_1,-\mu_1)/\mu_1 = \frac{\varpi}{2}p(-\mu_1,\mu_1)/\mu_1 = \varpi b/\mu_1.$$

Note that:

- We may interpret α and β as **local transmission and reflection coefficients**.

Accurate Numerical Solutions (16)

Four-stream approximation ($N = 2$):

$$
\begin{aligned}
\mu_1 \frac{dI^+(\tau,\mu_1)}{d\tau} &= I^+(\tau,\mu_1) - Q'^+(\tau,\mu_1) \\
&\quad - w_2\frac{\varpi}{2}p(-\mu_2,\mu_1)I^-(\tau,\mu_2) - w_1\frac{\varpi}{2}p(-\mu_1,\mu_1)I^-(\tau,\mu_1) \\
&\quad - w_1\frac{\varpi}{2}p(\mu_1,\mu_1)I^+(\tau,\mu_1) - w_2\frac{\varpi}{2}p(\mu_2,\mu_1)I^+(\tau,\mu_2) \\
\mu_2 \frac{dI^+(\tau,\mu_2)}{d\tau} &= I^+(\tau,\mu_2) - Q'^+(\tau,\mu_2) \\
&\quad - w_2\frac{\varpi}{2}p(-\mu_2,\mu_2)I^-(\tau,\mu_2) - w_1\frac{\varpi}{2}p(-\mu_1,\mu_2)I^-(\tau,\mu_1) \\
&\quad - w_1\frac{\varpi}{2}p(\mu_1,\mu_2)I^+(\tau,\mu_1) - w_2\frac{\varpi}{2}p(\mu_2,\mu_2)I^+(\tau,\mu_2) \\
-\mu_1 \frac{dI^-(\tau,\mu_1)}{d\tau} &= I^-(\tau,\mu_1) - Q'^-(\tau,\mu_1) \\
&\quad - w_2\frac{\varpi}{2}p(-\mu_2,-\mu_1)I^-(\tau,\mu_2) - w_1\frac{\varpi}{2}p(-\mu_1,-\mu_1)I^-(\tau,\mu_1) \\
&\quad - w_1\frac{\varpi}{2}p(\mu_1,-\mu_1)I^+(\tau,\mu_1) - w_2\frac{\varpi}{2}p(\mu_2,-\mu_1)I^+(\tau,\mu_2) \\
-\mu_2 \frac{dI^-(\tau,\mu_2)}{d\tau} &= I^-(\tau,\mu_2) - Q'^-(\tau,\mu_2) \\
&\quad - w_2\frac{\varpi}{2}p(-\mu_2,-\mu_2)I^-(\tau,\mu_2) - w_1\frac{\varpi}{2}p(-\mu_1,-\mu_2)I^-(\tau,\mu_1) \\
&\quad - w_1\frac{\varpi}{2}p(\mu_1,-\mu_2)I^+(\tau,\mu_1) - w_2\frac{\varpi}{2}p(\mu_2,-\mu_2)I^+(\tau,\mu_2).
\end{aligned}
$$

Accurate Numerical Solutions (17)

We may rewrite these equations in matrix form as follows:

$$\frac{d}{d\tau}\begin{bmatrix} I^+(\tau,\mu_1) \\ I^+(\tau,\mu_2) \\ I^-(\tau,\mu_1) \\ I^-(\tau,\mu_2) \end{bmatrix} = \begin{bmatrix} -\alpha_{11} & -\alpha_{12} & -\beta_{11} & -\beta_{12} \\ -\alpha_{21} & -\alpha_{22} & -\beta_{21} & -\beta_{22} \\ \beta_{11} & \beta_{12} & \alpha_{11} & \alpha_{12} \\ \beta_{21} & \beta_{22} & \alpha_{21} & \alpha_{22} \end{bmatrix} \begin{bmatrix} I^+(\tau,\mu_1) \\ I^+(\tau,\mu_2) \\ I^-(\tau,\mu_1) \\ I^-(\tau,\mu_2) \end{bmatrix} - \begin{bmatrix} Q^+(\tau,\mu_1) \\ Q^+(\tau,\mu_2) \\ Q^-(\tau,\mu_1) \\ Q^-(\tau,\mu_2) \end{bmatrix} \tag{69}$$

where

$$\begin{aligned}
Q^{\pm}(\tau,\mu_i) &= \pm\mu_i^{-1}Q'^{\pm}(\tau,\mu_i), \qquad i = 1,2, \\
\alpha_{11} &= \mu_1^{-1}[w_1\frac{\varpi}{2}p(\mu_1,\mu_1) - 1] = \mu_1^{-1}[w_1\frac{\varpi}{2}p(-\mu_1,-\mu_1) - 1], \\
\alpha_{12} &= \mu_1^{-1}w_2\frac{\varpi}{2}p(\mu_2,\mu_1) = \mu_1^{-1}w_2\frac{\varpi}{2}p(-\mu_2,-\mu_1), \\
\alpha_{21} &= \mu_2^{-1}w_1\frac{\varpi}{2}p(\mu_1,\mu_2) = \mu_2^{-1}w_1\frac{\varpi}{2}p(-\mu_1,-\mu_2), \\
\alpha_{22} &= \mu_2^{-1}[w_2\frac{\varpi}{2}p(\mu_2,\mu_2) - 1] = \mu_2^{-1}[w_2\frac{\varpi}{2}p(-\mu_2,-\mu_2) - 1], \\
\beta_{11} &= \mu_1^{-1}w_1\frac{\varpi}{2}p(\mu_1,-\mu_1) = \mu_1^{-1}w_1\frac{\varpi}{2}p(-\mu_1,\mu_1), \\
\beta_{12} &= \mu_1^{-1}w_2\frac{\varpi}{2}p(-\mu_2,\mu_1) = \mu_1^{-1}w_2\frac{\varpi}{2}p(\mu_2,-\mu_1), \\
\beta_{21} &= \mu_2^{-1}w_1\frac{\varpi}{2}p(-\mu_1,\mu_2) = \mu_2^{-1}w_1\frac{\varpi}{2}p(\mu_1,-\mu_2), \\
\beta_{22} &= \mu_2^{-1}w_2\frac{\varpi}{2}p(-\mu_2,\mu_2) = \mu_2^{-1}w_2\frac{\varpi}{2}p(\mu_2,-\mu_2).
\end{aligned}$$

Accurate Numerical Solutions (18)

By introducing the vectors:

$$\mathbf{I}^{\pm} = \left\{ I^{\pm}(\tau, \mu_i) \right\}, \qquad \mathbf{Q}^{\pm} = \{ Q^{\pm}(\tau, \mu_i) \}, \qquad i = 1, 2$$

we may write Eq. 69 in a more compact form as:

$$\frac{d}{d\tau} \begin{bmatrix} \mathbf{I}^{+} \\ \mathbf{I}^{-} \end{bmatrix} = \begin{bmatrix} -\tilde{\alpha} & -\tilde{\beta} \\ \tilde{\beta} & \tilde{\alpha} \end{bmatrix} \begin{bmatrix} \mathbf{I}^{+} \\ \mathbf{I}^{-} \end{bmatrix} - \begin{bmatrix} \mathbf{Q}^{+} \\ \mathbf{Q}^{-} \end{bmatrix} \tag{70}$$

where all the elements of the matrices $\tilde{\alpha}$ and $\tilde{\beta}$ are defined above.

Note that:

- Equation 70 is similar to the one obtained in the two-stream approximation except that the scalars α and β have become 2×2 matrices.
- $\tilde{\alpha}$ and $\tilde{\beta}$ may be interpreted as **local transmission and reflection operators**.

Accurate Numerical Solutions (19)

Multi-stream approximation (N arbitrary):

It should now be obvious how to generalize this scheme:

- We write Eqs. 63 and 64 in matrix form as:

$$\frac{d}{d\tau}\begin{bmatrix}\mathbf{I}^+\\ \mathbf{I}^-\end{bmatrix} = \begin{bmatrix}-\tilde{\alpha} & -\tilde{\beta}\\ \tilde{\beta} & \tilde{\alpha}\end{bmatrix}\begin{bmatrix}\mathbf{I}^+\\ \mathbf{I}^-\end{bmatrix} - \begin{bmatrix}\mathbf{Q}^+\\ \mathbf{Q}^-\end{bmatrix} \tag{71}$$

where

$$\begin{aligned}
\mathbf{I}^{\pm} &= \{I^{\pm}(\tau,\mu_i)\} \qquad i = 1,\ldots,N\\
\mathbf{Q}^{\pm} &= \pm\mathbf{M}^{-1}\mathbf{Q}'^{\pm} = \{Q^{\pm}(\tau,\mu_i)\} \qquad i = 1,\ldots,N\\
\mathbf{M} &= \{\mu_i\delta_{ij}\} \qquad i,j = 1,\ldots,N\\
\tilde{\alpha} &= \mathbf{M}^{-1}\{\mathbf{D}^+\mathbf{W} - \mathbf{1}\}\\
\tilde{\beta} &= \mathbf{M}^{-1}\mathbf{D}^-\mathbf{W}\\
\mathbf{W} &= \{w_i\delta_{ij}\} \qquad i,j = 1,\ldots,N\\
\mathbf{1} &= \{\delta_{ij}\} \qquad i,j = 1,\ldots,N\\
\mathbf{D}^+ &= \frac{\varpi}{2}\{p(\mu_j,\mu_i)\} = \frac{\varpi}{2}\{p(-\mu_j,-\mu_i)\} \qquad i,j = 1,\ldots,N\\
\mathbf{D}^- &= \frac{\varpi}{2}\{p(-\mu_j,\mu_i)\} = \frac{\varpi}{2}\{p(\mu_j,-\mu_i)\} \qquad i,j = 1,\ldots,N.
\end{aligned}$$

Accurate Numerical Solutions (20)

We note that the structure of the $(2N \times 2N)$ matrix:

$$\begin{bmatrix} -\tilde{\alpha} & -\tilde{\beta} \\ \tilde{\beta} & \tilde{\alpha} \end{bmatrix}$$

in Eq. 71 can be traced to:

- the dependence of the scattering phase function on only the scattering angle (i.e. the angle between $\hat{\Omega}(\mu, \phi)$ and $\hat{\Omega}(\mu', \phi')$.
- This special structure is also a consequence of having chosen a quadrature rule satisfying $\mu_{-i} = -\mu_i$, $w_{-i} = w_i$.
- Because of this structure, Eq. 71 permits eigensolutions with eigenvalues occurring in positive/negative pairs:
- We can reduce the dimension of the resulting algebraic eigenvalue problem by a factor of 2 which leads to a decrease of the computational burden by a factor of 8.

Accurate Numerical Solutions (21)

Matrix Eigensolutions

Two-stream solutions ($N = 1$):

- Seeking solutions to the homogeneous version of Eq. 68 ($Q^{\pm} = 0$) of the form $I^{\pm} = g^{\pm} e^{-\lambda\tau}$, $g^{\pm} = g(\pm\mu_1)$, leads to the algebraic eigenvalue problem:

$$\begin{bmatrix} \alpha & \beta \\ -\beta & -\alpha \end{bmatrix} \begin{bmatrix} g^+ \\ g^- \end{bmatrix} = \lambda \begin{bmatrix} g^+ \\ g^- \end{bmatrix}. \tag{72}$$

Writing this matrix equation as follows:

$$\begin{aligned} \alpha g^+ + \beta g^- &= \lambda g^+ \\ -\beta g^+ - \alpha g^- &= \lambda g^- \end{aligned}$$

and adding and subtracting these two equations, we find:

$$(\alpha - \beta)(g^+ - g^-) = \lambda(g^+ + g^-) \tag{73}$$

$$(\alpha + \beta)(g^+ + g^-) = \lambda(g^+ - g^-). \tag{74}$$

Accurate Numerical Solutions (22)

Substitution of the last equation into Eq. 73 yields:

$$(\alpha - \beta)(\alpha + \beta)(g^+ + g^-) = \lambda^2 (g^+ + g^-)$$

which has the solutions $\lambda_1 = k$, $\lambda_{-1} = -k$ with

$$k = \sqrt{\alpha^2 - \beta^2} = \frac{1}{\mu_1}\sqrt{(1-\varpi)(1-\varpi+2\varpi b)} > 0 \qquad (\varpi < 1) \tag{75}$$

$$g^+ + g^- = \text{arbitrary constant} \qquad (= 1) \tag{76}$$

which we may set equal to unity.

For $\lambda_1 = k$ Eq. 74 yields:

$$g^+ - g^- = (\alpha + \beta)/k \tag{77}$$

(assuming $k \neq 0$ or $\varpi \neq 1$).

Accurate Numerical Solutions (23)

- Combining Eqs. 76 and 77, we find:

$$\frac{g_1^+}{g_1^-} = \frac{k + (\alpha + \beta)}{k - (\alpha + \beta)} = \frac{\sqrt{1 - \varpi + 2\varpi b} - \sqrt{1 - \varpi}}{\sqrt{1 - \varpi + 2\varpi b} + \sqrt{1 - \varpi}} \equiv \rho_\infty \tag{78}$$

and thus

$$\begin{bmatrix} g_1^+ \\ g_1^- \end{bmatrix} = \begin{bmatrix} \rho_\infty \\ 1 \end{bmatrix} \tag{79}$$

which is the eigenvector belonging to eigenvalue $\lambda_1 = k$.

- Repeating this procedure for $\lambda_{-1} = -k$, we find $g_{-1}^- / g_{-1}^+ = \rho_\infty$, and:

$$\begin{bmatrix} g_{-1}^+ \\ g_{-1}^- \end{bmatrix} = \begin{bmatrix} 1 \\ \rho_\infty \end{bmatrix}. \tag{80}$$

Accurate Numerical Solutions (24)

The complete homogeneous solution becomes a linear combination of the exponential solutions for eigenvalues $\lambda_1 = k$ and $\lambda_{-1} = -k$, i.e.

$$\begin{aligned} I^+(\tau) &= I(\tau, +\mu_1) = C_{-1}g_{-1}(+\mu_1)e^{+k\tau} + C_1 g_1(+\mu_1)e^{-k\tau} \\ &= C_{-1}g_{-1}(+\mu_1)e^{+k\tau} + \rho_\infty C_1 g_1(-\mu_1)e^{-k\tau} \qquad (81) \\ I^-(\tau) &= I(\tau, -\mu_1) = C_{-1}g_{-1}(-\mu_1)e^{+k\tau} + C_1 g_1(-\mu_1)e^{-k\tau} \\ &= \rho_\infty C_{-1}g_{-1}(+\mu_1)e^{+k\tau} + C_1 g_1(-\mu_1)e^{-k\tau} \qquad (82) \end{aligned}$$

where C_1 and C_{-1} are constants of integration. We note that:

- These solutions are identical to those given previously (see Chapter 7) for the two-stream approximation as they should be.
- In anticipation of the extension to more than two streams we may rewrite the solution in the following somewhat artificial form:

$$I^\pm(\tau, \mu_i) = \sum_{j=1}^{1} C_{-j}g_{-j}(\pm\mu_i)e^{k_j\tau} + \sum_{j=1}^{1} C_j g_j(\pm\mu_i)e^{-k_j\tau} \qquad i = 1, 1 \qquad (83)$$

with $k_1 = k$, given by Eq. 75.

Accurate Numerical Solutions (25)

Multi-stream solutions (N arbitrary)

The coupled Eqs. 71: $\frac{d}{d\tau}\begin{bmatrix}\mathbf{I}^+\\ \mathbf{I}^-\end{bmatrix} = \begin{bmatrix}-\tilde{\alpha} & -\tilde{\beta}\\ \tilde{\beta} & \tilde{\alpha}\end{bmatrix}\begin{bmatrix}\mathbf{I}^+\\ \mathbf{I}^-\end{bmatrix} - \begin{bmatrix}\mathbf{Q}^+\\ \mathbf{Q}^-\end{bmatrix}$ constitue:

- a system of $2N$ coupled, ordinary differential equations with constant coefficients.
- These coupled equations are linear and our goal is to uncouple them by using well-known methods of linear algebra.
- Our discussion of the two- and four-stream cases suggest that we should proceed by seeking solutions to the homogeneous version ($\mathbf{Q} = 0$) of the form:

$$\mathbf{I}^{\pm} = \mathbf{g}^{\pm} e^{-k\tau}. \tag{84}$$

We find:

$$\begin{bmatrix}\tilde{\alpha} & \tilde{\beta}\\ -\tilde{\beta} & -\tilde{\alpha}\end{bmatrix}\begin{bmatrix}\mathbf{g}^+\\ \mathbf{g}^-\end{bmatrix} = k\begin{bmatrix}\mathbf{g}^+\\ \mathbf{g}^-\end{bmatrix}. \tag{85}$$

- Equation 85 is a standard algebraic eigenvalue problem of dimension $2N \times 2N$ with eigenvalues k and eigenvectors $\mathbf{g}^{\pm}$.

Accurate Numerical Solutions (26)

Because of the special structure of the matrix in Eq. 85:

- the eigenvalues occur in positive/negative pairs and the dimension of the algebraic eigenvalue problem (Eq. 85) may be reduced as follows:

We rewrite the homogeneous version of Eq. 71 as:

$$\frac{d\mathbf{I}^+}{d\tau} = -\tilde{\alpha}\mathbf{I}^+ - \tilde{\beta}\mathbf{I}^-$$
$$\frac{d\mathbf{I}^-}{d\tau} = \tilde{\alpha}\mathbf{I}^- + \tilde{\beta}\mathbf{I}^+.$$

Adding these two equations, we find:

$$\frac{d(\mathbf{I}^+ + \mathbf{I}^-)}{d\tau} = -(\tilde{\alpha} - \tilde{\beta})(\mathbf{I}^+ - \mathbf{I}^-) \tag{86}$$

and subtracting them, we find:

$$\frac{d(\mathbf{I}^+ - \mathbf{I}^-)}{d\tau} = -(\tilde{\alpha} + \tilde{\beta})(\mathbf{I}^+ + \mathbf{I}^-). \tag{87}$$

Accurate Numerical Solutions (27)

Combining Eqs. 86 and 87, we obtain:

$$\frac{d^2(\mathbf{I}^+ + \mathbf{I}^-)}{d\tau^2} = (\tilde{\alpha} - \tilde{\beta})(\tilde{\alpha} + \tilde{\beta})(\mathbf{I}^+ + \mathbf{I}^-)$$

or in view of Eq. 84:

$$(\tilde{\alpha} - \tilde{\beta})(\tilde{\alpha} + \tilde{\beta})(\mathbf{g}^+ + \mathbf{g}^-) = k^2(\mathbf{g}^+ + \mathbf{g}^-). \qquad (88)$$

- Note reduction of dimension from $2N$ to N [$(\tilde{\alpha} - \tilde{\beta})(\tilde{\alpha} + \tilde{\beta})$ has dimension N].
- To proceed we solve Eq. 88 to obtain eigenvalues and eigenvectors $(\mathbf{g}^+ + \mathbf{g}^-)$.
- We then use Eq. 87 to determine $(\mathbf{g}^+ - \mathbf{g}^-)$, and proceed as in the four-stream case to construct a complete set of eigenvectors.

Inhomogeneous Solution

- It is easily verified that a particular solution for collimated beam incidence is:

$$I(\tau, u_i) = Z_0(u_i)e^{-\tau/\mu_0}. \qquad (89)$$

Accurate Numerical Solutions (28)

The $Z_0(u_i)$ are determined by the following system of **linear algebraic** equations:

$$\sum_{\substack{j=-N \\ j\neq 0}}^{N} \left[(1 + u_j/\mu_0)\delta_{ij} - w_j \frac{\varpi}{2} p(u_j, u_i) \right] Z_0(u_j) = X_0(u_i). \tag{90}$$

Equation 90 is obtained by substituting the "trial" solution Eq. 89 into Eqs. 63–64.

Thermal Source

For thermal sources the emitted radiation is isotropic (and azimuth-independent):

$$Q'(\tau) = (1 - \varpi)B(\tau).$$

To account for the temperature variation in the slab we may approximate the Planck function for each layer by a polynomial in optical depth τ:

$$B[T(\tau)] = \sum_{\ell=0}^{K} b_\ell \tau^\ell.$$

- Then, we assume that the solution should also be a polynomial in τ, i.e.

$$I(\tau, u_i) = \sum_{\ell=0}^{K} Y_\ell(u_i)\tau^\ell.$$

Accurate Numerical Solutions (29)

The $Y_\ell(u_i)$ are determined by solving this system of linear algebraic equations:

$$
\begin{aligned}
Y_K(u_i) &= (1-\varpi)b_K \\
\sum_{j=-N}^{N} \left(\delta_{ij} - w_j \frac{\varpi}{2} p(u_j, u_i)\right) Y_\ell(u_j) &= (1-\varpi)b_\ell - (\ell+1)u_i Y_{\ell+1}(u_i) \\
&\quad \ell = K-1, K-2, \ldots, 0.
\end{aligned}
$$

- $K = 1$: only requires T at layer interfaces to compute $B(\tau)$ there.

General Solution

The general solution to Eqs. 63 and 64 consists of a linear combination, with coefficients C_j, of all the homogeneous solutions, plus the particular solution:

$$
\begin{aligned}
I^{\pm}(\tau, \mu_i) &= \sum_{j=1}^{N} C_{-j} g_{-j}(\pm\mu_i) e^{k_j \tau} + \sum_{j=1}^{N} C_j g_j(\pm\mu_i) e^{-k_j \tau} \\
&\quad + Z_0(\pm\mu_i) e^{-\tau/\mu_0} \qquad i = 1, \ldots, N.
\end{aligned} \tag{91}
$$

- The k_j and $g_j(\pm\mu_i)$ are the eigenvalues and eigenvectors; the $\pm\mu_i$ are the quadrature angles; the $C_{\pm j}$ the constants of integration.

Accurate Numerical Solutions (30)

Boundary Conditions – Removal of Ill-Conditioning

Boundary Conditions

- If the diffuse bidirectional reflectance, $\rho_{\rm d}(\mu, \phi; -\mu', \phi')$, is a function only of the difference between the azimuthal angles before and after reflection, then:

$$\rho_{\rm d}(-\mu', \phi'; \mu, \phi) = \rho_{\rm d}(-\mu', \mu; \phi - \phi') = \sum_{m=0}^{2N-1} \rho_{\rm d}^m(-\mu', \mu) \cos m(\phi - \phi')$$

where the expansion coefficients are computed from:

$$\rho_{\rm d}^m(-\mu', \mu) = \frac{1}{\pi} \int_{-\pi}^{\pi} d(\phi - \phi') \rho_{\rm d}(-\mu', \mu; \phi - \phi') \cos m(\phi - \phi').$$

- Each Fourier component must satisfy the bottom boundary condition ($T_{\rm s}$ is temperature, and $\epsilon(\mu)$ emittance of the surface):

$$I^m(\tau^*, +\mu) \; = \; \delta_{m0}\epsilon(\mu)B(T_{\rm s}) + (1 + \delta_{m0}) \int_0^1 d\mu' \, \mu' \rho_{\rm d}^m(-\mu', \mu) I^m(\tau^*, -\mu') + \frac{\mu_0 F^{\rm s}}{\pi} e^{-\tau^*/\mu_0} \rho_{\rm d}^m(\mu, -\mu_0) \equiv I_{\rm s}^m(\mu).$$

Accurate Numerical Solutions (31)

Thus, Eqs. 91 must satisfy boundary conditions as follows:

$$I^m(0, -\mu_i) = \mathcal{I}^m(-\mu_i), \qquad i = 1, \ldots, N \tag{92}$$

$$I^m(\tau^*, +\mu_i) = I_{\rm s}^m(\mu_i), \qquad i = 1, \ldots, N \tag{93}$$

where

$$\begin{aligned} I_{\rm s}^m(\mu_i) \;=\; & \delta_{m0}\epsilon(\mu_i)B(T_{\rm s}) + (1+\delta_{m0})\sum_{j=1}^{N} w_j\mu_j\rho_{\rm d}^m(\mu_i, -\mu_j)I^m(\tau^*, -\mu_j) \\ & + \frac{\mu_0 F^{\rm s}}{\pi}e^{-\tau^*/\mu_0}\rho_{\rm d}^m(\mu_i, -\mu_0). \end{aligned} \tag{94}$$

$\mathcal{I}^m(-\mu_i)$ is the radiation incident at the top boundary.

Note that:

- For *Prototype Problem 1* we would have $\mathcal{I}^m(-\mu_i) =$ constant (the same for all μ_i) for $m = 0$, and $\mathcal{I}^m(-\mu_i) = 0$ for $m \neq 0$ (uniform illumination).
- For **Prototype Problems 2 and 3** we have, of course, $\mathcal{I}^m(-\mu_i) = 0$ since there is by definition no diffuse radiation incident in **Prototype Problem 3** and **Prototype Problem 2** is assumed to be driven entirely by internal radiation sources.

Accurate Numerical Soln's – Prototype Problems (32)

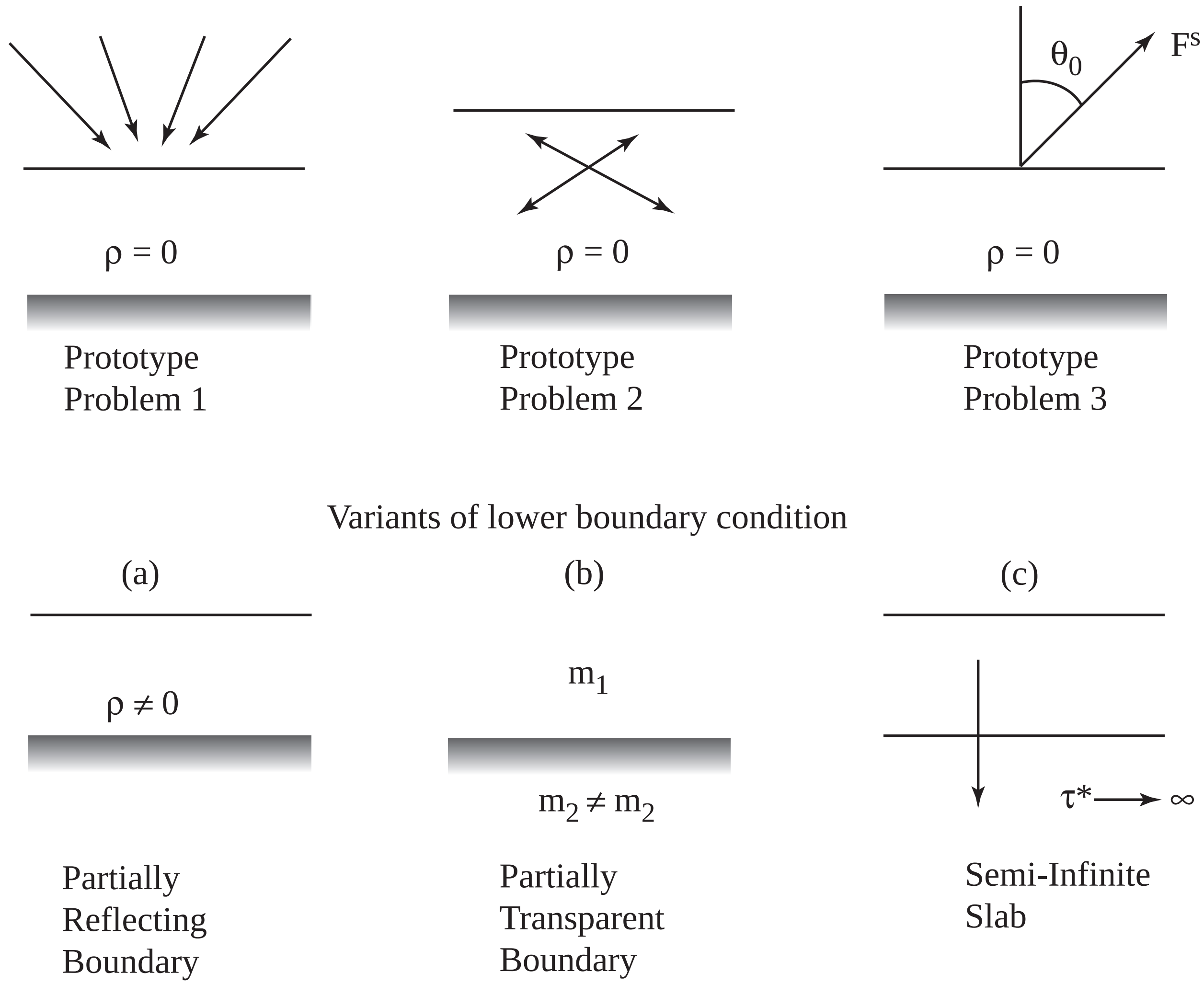

Figure 8: **Illustration of Prototype Problems in radiative transfer.**

Accurate Numerical Solutions (33)

Note also that since Eqs. 92 and 93 introduce:

- a fundamental distinction between downward directions (denoted by $-$) and upward directions (denoted by $+$), one should select a quadrature rule which integrates separately over the downward and upward directions.
- The Double-Gauss rule that we have adopted satisfies this requirement.

For the discussion of boundary conditions, it is convenient to write the discrete ordinate solution in the following form ($k_j > 0$ and $k_{-j} = -k_j$):

$$I^{\pm}(\tau, \mu_i) = \sum_{j=1}^{N} \left[C_j g_j(\pm\mu_i) e^{-k_j \tau} + C_{-j} g_{-j}(\pm\mu_i) e^{+k_j \tau} \right] + U^{\pm}(\tau, \mu_i). \qquad (95)$$

Here:

- The sum contains the homogeneous solution involving the unknown coefficients (the C_j) and
- $U^{\pm}(\tau, \mu_i)$ is the particular solution given by Eq. 89.

Accurate Numerical Solutions (34)

Insertion of Eq. 95 into Eqs. 92–94 yields (omitting the m-superscript):

$$\sum_{j=1}^{N} \{C_j g_j(-\mu_i) + C_{-j} g_{-j}(-\mu_i)\} = \mathcal{I}(-\mu_i) - U^-(0, \mu_i), \qquad i = 1, \ldots, N \quad (96)$$

$$\sum_{j=1}^{N} \left\{C_j r_j(\mu_i) g_j(+\mu_i) e^{-k_j \tau^*} + C_{-j} r_{-j}(\mu_i) g_{-j}(+\mu_i) e^{k_j \tau^*}\right\} = \Gamma(\tau^*, \mu_i),$$
$$i = 1, \ldots, N \quad (97)$$

where

$$r_j(\mu_i) = 1 - (1 + \delta_{m0}) \sum_{n=1}^{N} \rho_{\rm d}(\mu_i, -\mu_n) w_n \mu_n g_j(-\mu_n)/g_j(+\mu_i) \quad (98)$$

$$\begin{aligned}\Gamma(\tau^*, \mu_i) \; = \; & \delta_{m0}\, \epsilon(\mu_i) B(T_{\rm s}) - U^+(\tau^*, \mu_i) \\ & + (1 + \delta_{m0}) \sum_{j=1}^{N} \rho_{\rm d}(\mu_i, -\mu_j) w_j \mu_j U^-(\tau^*, \mu_j) \\ & + \frac{\mu_0 F^{\rm s}}{\pi} e^{-\tau^*/\mu_0} \rho_{\rm d}(\mu_i, -\mu_0). \end{aligned} \quad (99)$$

Accurate Numerical Solutions (35)

Note that:

- Eqs. 96 and 97 constitute a $2N \times 2N$ system of linear algebraic equations from which the $2N$ unknown coefficients, the C_j ($j = \pm 1, \ldots, \pm N$) are determined.

Removal of Numerical Ill-Conditioning

- The numerical solution of this set of equations is seriously hampered by the fact that Eqs. 96 and 97 are intrinsically ill-conditioned.

By "ill-conditioning" we mean:

- When Eqs. 96 and 97 are written in matrix form the resulting matrix cannot be successfully inverted by existing computers using "finite-digit" arithmetic.
- If τ^* is sufficiently large, some of the elements of the matrix become huge while others become tiny: **this situation leads to ill-conditioning**.
- Fortunately, this ill-conditioning may be eliminated by a scaling transformation.
- The ill-conditioning is due to the occurrence of exponentials with positive arguments in Eqs. 96 and 97 (recall that $k_j > 0$) which must be removed.

Accurate Numerical Solutions (36)

- The ill-conditioning is removed by applying the scaling transformation:

$$C_{+j} = C'_{+j} e^{k_j \tau_t} \qquad \text{and} \qquad C_{-j} = C'_{-j} e^{-k_j \tau_b}. \tag{100}$$

To generalize this scaling to apply to a multi-layered medium we have written:

- τ_t and τ_b for the optical depths at the top and the bottom of the layer, respectively. In the present one-layer case we have $\tau_t = 0$ and $\tau_b = \tau^*$.

Using Eqs. 100 in Eqs. 96 and 97 and solving for the C'_j instead of the C_j:

- All the exponential terms in the coefficient matrix have negative arguments ($k_j > 0, \tau_b > \tau_t$). Consequently:
- Numerical ill-conditioning is avoided: the system of algebraic equations determining the C'_j will be unconditionally stable for arbitrary layer thickness.
- The merit of the scaling transformation is to remove all positive arguments of the exponentials occurring in the matrix elements of the coefficient matrix.

BUT HOW DOES IT WORK?

Accurate Numerical Solutions (37)

Example: Removal of Ill-Conditioning – Two-Stream Case ($N = 1$)

In this simple case, Eqs. 96 and 97 reduce to: (see Eqs. 81 and 82)

$$C_1 g_1(-\mu_1)e^{-k\tau_t} + C_{-1}g_{-1}(-\mu_1)e^{k\tau_t} = C_1 g_1^- e^{-k\tau_t} + C_{-1}g_{-1}^- e^{k\tau_t} = (RHS)_t$$

$$r_1 C_1 g_1(+\mu_1)e^{-k\tau_b} + r_{-1}C_{-1}g_{-1}(+\mu_1)e^{k\tau_b} = r_1 C_1 g_1^+ e^{-k\tau_b} + r_{-1}C_{-1}g_{-1}^+ e^{k\tau_b} = (RHS)_b$$

The left hand side may be written in matrix form as:

$$\begin{bmatrix} g_1^- e^{-k\tau_t} & g_{-1}^- e^{k\tau_t} \\ r_1 g_1^+ e^{-k\tau_b} & r_{-1}g_{-1}^+ e^{k\tau_b} \end{bmatrix} \begin{bmatrix} C_1 \\ C_{-1} \end{bmatrix}.$$

This matrix is ill-conditioned because: One element becomes very large while another one becomes very small as $k\tau_b$ increases. Using the scaling transformation we find that the above matrix becomes:

$$\begin{bmatrix} g_1^- & g_{-1}^- e^{-k(\tau_b-\tau_t)} \\ r_1 g_1^+ e^{-k(\tau_b-\tau_t)} & r_{-1}g_{-1}^+ \end{bmatrix} \begin{bmatrix} C_1' \\ C_{-1}' \end{bmatrix}.$$

In the limit of large values of $k(\tau_b - \tau_t)$ this matrix reduces to:

$$\begin{bmatrix} g_1^- & 0 \\ 0 & r_{-1}g_{-1}^+ \end{bmatrix}.$$

- **The ill-conditioning problem has been completely eliminated.**

2.10.3 Two-stream, two-layer case (N=1, L=2)

Proceeding as in the one-layer case above, we write the left-hand side of (46) out explicitly in the two-stream approximation for a two-layer medium as follows:

$$C_{1,1}G_{1,1}(-\mu_1)+C_{-1,1}G_{-1,1}(-\mu_1)=(\mathrm{RHS})_1$$

$$C_{1,1}G_{1,1}(-\mu_1)e^{-k_1\tau_1}+C_{-1,1}G_{-1,1}(-\mu_1)e^{k_1\tau_1}-C_{1,2}G_{1,2}(-\mu_1)e^{-k_2\tau_1}-C_{-1,2}G_{-1,2}(-\mu_1)e^{k_2\tau_1}=(\mathrm{RHS}$$

$$C_{1,1}G_{1,1}(+\mu_1)e^{-k_1\tau_1}+C_{-1,1}G_{-1,1}(+\mu_1)e^{k_1\tau_1}-C_{1,2}G_{1,2}(+\mu_1)e^{-k_2\tau_1}-C_{-1,2}G_{-1,2}(+\mu_1)e^{k_2\tau_1}=(\mathrm{RHS}$$

$$r_{1,2}C_{1,2}G_{1,2}(+\mu_1)e^{-k_2\tau_2}+r_{-1,2}C_{-1,2}G_{-1,2}(+\mu_1)e^{k_2\tau_2}=(\mathrm{RHS})_4$$

Using (20b) and (20c), we may write the left hand sides of the above equations in matrix form as

$$\begin{bmatrix} 1 & R_1 & 0 & 0 \\ e^{-k_1\tau_1} & R_1e^{k_1\tau_1} & -e^{-k_2\tau_1} & -R_2e^{k_2\tau_1} \\ R_1e^{-k_1\tau_1} & e^{k_1\tau_1} & -R_2e^{-k_2\tau_1} & -e^{k_2\tau_1} \\ 0 & 0 & R_2r_{1,2}e^{-k_2\tau_2} & r_{-1,2}e^{k_2\tau_2} \end{bmatrix}\begin{bmatrix} C_{1,1} \\ C_{-1,1} \\ C_{1,2} \\ C_{-1,2} \end{bmatrix}$$

Introducing the scaling transformation (48), we obtain

$$\begin{bmatrix} 1 & R_1e^{-k_1\tau_1} & 0 & 0 \\ e^{-k_1\tau_1} & R_1 & -1 & -R_2e^{-k_2(\tau_2-\tau_1)} \\ R_1e^{-k_1\tau_1} & 1 & -R_2 & -e^{-k_2(\tau_2-\tau_1)} \\ 0 & 0 & R_2r_{1,2}e^{-k_2(\tau_2-\tau_1)} & r_{-1,2} \end{bmatrix}\begin{bmatrix} \hat{C}_{1,1} \\ \hat{C}_{-1,1} \\ \hat{C}_{1,2} \\ \hat{C}_{-1,2} \end{bmatrix} \tag{49}$$

$$\begin{bmatrix} 1 & 0 & 0 & 0 \\ 0 & R_1 & -1 & 0 \\ 0 & 1 & -R_2 & 0 \\ 0 & 0 & 0 & r_{-1,2} \end{bmatrix}$$

Accurate Numerical Soln's – Inhomogeneous Slab (38)

So far we have considered only a **homogeneous slab:** the **single scattering albedo** and the **scattering phase function** were assumed to be constant throughout the slab. We shall now allow for both to be a function of optical depth:

- To approximate the behavior of a vertically inhomogeneous slab we will divide it into a number of layers. Thus:
- the slab is assumed to consist of L adjacent layers in which the single scattering albedo and the scattering phase function are taken to be constant within each layer, **but are allowed to vary from layer to layer.**
- For an emitting slab we assume that we know the temperature at the layer boundaries.
- The idea is that **by using enough layers we can approximate the actual variation in optical properties and temperature as closely as desired.**
- The advantage of this approach is that we can use the solutions derived previously because each of the layers by assumption is homogeneous.

Accurate Numerical Soln's – Multiple Layers (39)

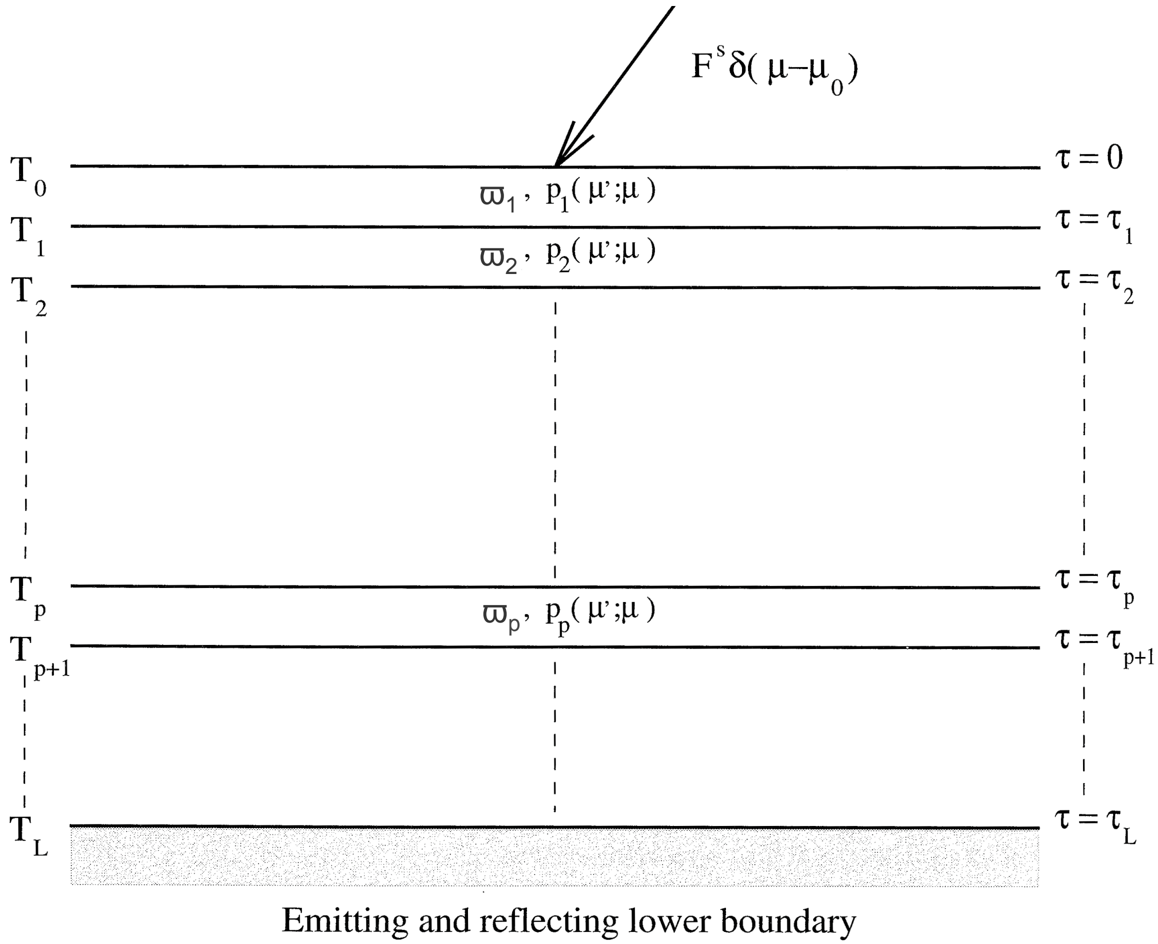

Figure 9: **Schematic illustration of a multi-layered, inhomogeneous medium overlying an emitting and partially reflecting surface.**

Accurate Numerical Soln's – Inhomogeneous Slab (40)

- Thus, we may write the solution for the p^{th} layer as ($k_{jp} > 0$ and $k_{-jp} = -k_{jp}$)

$$I_p^{\pm}(\tau, \mu_i) = \sum_{j=1}^{N} \left[C_{jp} g_{jp}(\pm\mu_i) e^{-k_{jp}\tau} + C_{-jp} g_{-jp}(\pm\mu_i) e^{+k_{jp}\tau} \right] + U_p^{\pm}(\tau, \mu_i)$$
$$p = 1, 2, \ldots, L. \qquad (101)$$

- The sum contains the homogeneous solution involving the unknown coefficients (the C_{jp}) and $U_p^{\pm}(\tau, \mu_i)$ is the particular solution given by Eq. 89.
- Except for the layer index p, Eq. 101 is identical to Eq. 95. The solution contains $2N$ constants per layer yielding a total of $2N \times L$ unknown constants.
- Now, Eq. 91 must now satisfy boundary and continuity conditions as follows:

$$I_1^m(0, -\mu_i) = \mathcal{I}^m(-\mu_i), \qquad i = 1, \ldots, N \qquad (102)$$
$$I_p^m(\tau_p, \mu_i) = I_{p+1}^m(\tau_p, \mu_i), \qquad i = \pm 1, \ldots, \pm N;\ p = 1, \ldots, L-1 \qquad (103)$$
$$I_L^m(\tau_L, +\mu_i) = I_{\mathrm{s}}^m(\mu_i), \qquad i = 1, \ldots, N \qquad (104)$$

- $I_{\mathrm{s}}^m(\mu_i)$ is given by Eq. 94 with τ^* replaced by τ_L.
- Equation 103 ensures that the radiance is continuous across layer interfaces.

Accurate Numerical Soln's – Inhomogeneous Slab (41)

Insertion of Eq. 101 into Eqs. 102–104 yields (omitting the m-superscript):

$$\sum_{j=1}^{N} \{C_{j1}g_{j1}(-\mu_i) + C_{-j1}g_{-j1}(-\mu_i)\} = \mathcal{I}(-\mu_i) - U_1(0, -\mu_i), \qquad i = 1, \ldots, N \tag{105}$$

$$\begin{aligned} &\sum_{j=1}^{N} \{C_{jp}g_{jp}(\mu_i)e^{-k_{jp}\tau_p} + C_{-jp}g_{-jp}(\mu_i)e^{k_{jp}\tau_p} \\ &\quad - \left[C_{j,p+1}g_{j,p+1}(\mu_i)e^{-k_{j,p+1}\tau_p} + C_{-j,p+1}g_{-j,p+1}(\mu_i)e^{k_{j,p+1}\tau_p}\right]\} = \\ &\qquad U_{p+1}(\tau_p, \mu_i) - U_p(\tau_p, \mu_i), \\ &\qquad i = \pm 1, \ldots, \pm N; p = 1, \ldots, L-1 \end{aligned} \tag{106}$$

$$\begin{aligned} \sum_{j=1}^{N} \left\{C_{jL}r_j(\mu_i)g_{jL}(\mu_i)e^{-k_{jL}\tau_L} + C_{-jL}r_{-j}(\mu_i)g_{jL}(\mu_i)e^{k_{jL}\tau_L}\right\} \; &= \; \Gamma(\tau_L, \mu_i), \\ i = 1, \ldots, N \end{aligned} \tag{107}$$

where r_j is given by Eq. 98 with g_j replaced by g_{jL}, and Γ is given by Eq. 99 with $U^{\pm}$ replaced by $U_L^{\pm}$ and τ^* by τ_L.

Accurate Numerical Soln's – Inhomogeneous Slab (42)

Equations 105–107 constitute:

- a $(2N \times L) \times (2N \times L)$ system of linear algebraic equations from which the $2N \times L$ unknown coefficients, the C_{jp} $(j = \pm 1, \ldots, \pm N; p = 1, \ldots, L)$ are to be determined.

Note that:

- Eqs. 105 and 107 constitute the boundary conditions and are therefore identical to Eqs. 96 and 97 (again except for the layer indices);
- Eqs. 106 constitute the interface radiance continuity conditions.
- As in the one-layer case, we must deal with the fact that Eqs. 105–107 are intrinsically ill-conditioned.
- Again, this ill-conditioning is entirely eliminated by the scaling transformation introduced previously (Eqs. 100).

Accurate Numerical Solutions (43)

Source Function and Angular Distributions

For a slab of thickness τ^*, we may formally solve Eqs. 63 and 64 ($\mu > 0$):

$$I^+(\tau,\mu) = I^+(\tau^*,\mu)e^{-(\tau^*-\tau)/\mu} + \int_\tau^{\tau^*} \frac{dt}{\mu} S^+(t,\mu)e^{-(t-\tau)/\mu} \tag{108}$$

$$I^-(\tau,\mu) = I^-(0,\mu)e^{-\tau/\mu} + \int_0^{\tau} \frac{dt}{\mu} S^-(t,\mu)e^{-(\tau-t)/\mu}. \tag{109}$$

These two equations show that:

- If we know $S^\pm(t,\mu)$, we can find the intensity at arbitrary μ.

Analytic Expression for the Source Function

- In view of Eqs. 63 and 64 the discrete-ordinate approximation to the source function may be written as:

$$\begin{aligned} S^\pm(\tau,\mu) \; = \; & \frac{\varpi}{2}\sum_{i=1}^{N} w_i p(-\mu_i,\pm\mu) I^-(\tau,\mu_i) \\ & + \frac{\varpi}{2}\sum_{i=1}^{N} w_i p(+\mu_i,\pm\mu) I^+(\tau,\mu_i) + X_0^\pm(\mu)e^{-\tau/\mu_0}. \end{aligned} \tag{110}$$

Accurate Numerical Solutions (44)

Substituting the general solution of Eq. 91 into Eq. 110, we find:

$$S^{\pm}(\tau,\mu) = \sum_{j=1}^{N} C_{-j}\tilde{g}_{-j}(\pm\mu)e^{k_j\tau} + \sum_{j=1}^{N} C_j\tilde{g}_j(\pm\mu)e^{-k_j\tau} + \tilde{Z}_0^{\pm}(\mu)e^{-\tau/\mu_0} \tag{111}$$

where

$$\tilde{g}_j(\pm\mu) = \frac{a}{2}\sum_{i=1}^{N}\{w_i p(-\mu_i,\pm\mu)g_j(-\mu_i) + w_i p(+\mu_i,\pm\mu)g_j(+\mu_i)\} \tag{112}$$

$$\tilde{Z}_0^{\pm}(\mu) = \frac{a}{2}\sum_{i=1}^{N}\{w_i p(-\mu_i,\pm\mu)Z_0(-\mu_i) + w_i p(+\mu_i,\pm\mu)Z_0(+\mu_i)\} + X_0(\pm\mu). \tag{113}$$

Note that:

- Equations 112 and 113 are convenient analytic interpolation formulas for the $\tilde{g}_j(\pm\mu)$ and the $\tilde{Z}_0(\pm\mu)$.
- The fact that they are derived from the basic radiative transfer equation to which we are seeking solutions, indicates that these expressions may be superior to any other standard interpolation scheme.

Interpolated Intensities

Using Eqs. 111 in Eqs. 108 and 109, we find that for a layer of thickness τ^*, the radiances become:

$$\begin{aligned} I^+(\tau,\mu) &= I^+(\tau^*,\mu)e^{-(\tau^*-\tau)/\mu} \\ &+ \sum_{j=-N}^{N} C_j \frac{\tilde{g}_j(+\mu)}{1+k_j\mu}\left\{e^{-k_j\tau} - e^{-[k_j\tau^*+(\tau^*-\tau)/\mu]}\right\} \end{aligned} \tag{114}$$

$$I^-(\tau,\mu) = I^-(0,\mu)e^{-\tau/\mu} + \sum_{j=-N}^{N} C_j \frac{\tilde{g}_j(-\mu)}{1-k_j\mu}\left\{e^{-k_j\tau} - e^{-\tau/\mu}\right\} \tag{115}$$

- We have for convenience included the particular solution as the $j = 0$ term in the sum so that $C_0\tilde{g}_0(\pm\mu) \equiv \tilde{Z}_0(\pm\mu)$ and $k_0 \equiv 1/\mu_0$.
- The basic virtue of Eqs. 114 and 115 has been demonstrated numerically.

Accurate Numerical Soln's – Inhomogeneous Slab (46)

In a multi-layered medium we may evaluate the integral in Eqs. 108 and 109:

$$I^+(\tau,\mu) = I^+(\tau^*,\mu)e^{-(\tau^*-\tau)/\mu} + \int_\tau^{\tau^*} \frac{dt}{\mu} S^+(t,\mu)e^{-(t-\tau)/\mu} \tag{116}$$

$$I^-(\tau,\mu) = I^-(0,\mu)e^{-\tau/\mu} + \int_0^{\tau} \frac{dt}{\mu} S^-(t,\mu)e^{-(\tau-t)/\mu} \tag{117}$$

by integrating layer by layer as follows ($\tau_{p-1} \le \tau \le \tau_p$ and $\mu > 0$):

$$\begin{aligned} \int_\tau^{\tau_L} \frac{dt}{\mu} S^+(t,\mu)e^{-(t-\tau)/\mu} &= \int_\tau^{\tau_p} \frac{dt}{\mu} S_p^+(t,\mu)e^{-(t-\tau)/\mu} \\ &+ \sum_{n=p+1}^{L} \int_{\tau_{n-1}}^{\tau_n} \frac{dt}{\mu} S_n^+(t,\mu)e^{-(t-\tau)/\mu} \end{aligned} \tag{118}$$

$$\begin{aligned} \int_0^{\tau} \frac{dt}{\mu} S^-(t,\mu)e^{-(\tau-t)/\mu} &= \sum_{n=1}^{p-1} \int_{\tau_{n-1}}^{\tau_n} \frac{dt}{\mu} S_n^-(t,\mu)e^{-(\tau-t)/\mu} \\ &+ \int_{\tau_{p-1}}^{\tau} \frac{dt}{\mu} S_p^-(t,\mu)e^{-(\tau-t)/\mu}. \end{aligned} \tag{119}$$

Accurate Numerical Soln's – Inhomogeneous Slab (47)

Using Eq. 111 $[S^{\pm}(\tau,\mu) = \sum_{j=1}^{N} C_{-j}\tilde{g}_{-j}(\pm\mu)e^{k_j\tau} + \sum_{j=1}^{N} C_j\tilde{g}_j(\pm\mu)e^{-k_j\tau} + \tilde{Z}_0^{\pm}(\mu)e^{-\tau/\mu_0}]$ for $S_n^{\pm}(t,\mu)$ in each layer (properly indexed) in Eqs. 118 and 119, we find:

$$
\begin{aligned}
I_p^+(\tau,\mu) &= I^+(\tau_L,\mu)e^{-(\tau_L-\tau)/\mu} \\
&\quad + \sum_{n=p}^{L}\sum_{j=-N}^{N} C_{jn}\frac{\tilde{g}_{jn}(+\mu)}{1+k_{jn}\mu}[e^{-[k_{jn}\tau_{n-1}+(\tau_{n-1}-\tau)/\mu]} - e^{-[k_{jn}\tau_n+(\tau_n-\tau)/\mu]}]
\end{aligned}
\tag{120}
$$

with τ_{n-1} replaced by τ for $n = p$,

$$
\begin{aligned}
I_p^-(\tau,\mu) &= I^-(0,\mu)e^{-\tau/\mu} \\
&\quad + \sum_{n=1}^{p}\sum_{j=-N}^{N} C_{jn}\frac{\tilde{g}_{jn}(-\mu)}{1-k_{jn}\mu}[e^{-[k_{jn}\tau_n+(\tau-\tau_n)/\mu]} - e^{-[k_{jn}\tau_{n-1}+(\tau-\tau_{n-1})/\mu]}]
\end{aligned}
\tag{121}
$$

with τ_n replaced by τ for $n = p$.
For a single layer ($\tau_{n-1} = \tau$, $\tau_n = \tau_L = \tau^*$ in Eq. 120; $\tau_n = \tau$, $\tau_{n-1} = 0$ in Eq. 121), Eqs. 120 and 121 reduce to Eqs. 114 and 115 as they should.

Accurate Numerical Soln's – Inhomogeneous Slab (48)

Scaled Solutions

Equations 101 and 120 and 121 contain exponentials with positive arguments which will eventually lead to numerical overflow for large enough values of these arguments. Fortunately:

- we can remove all these positive arguments by introducing the scaling transformation into our solutions.

Since only the homogeneous solution is affected, it suffices to substitute Eqs. 100 into the homogeneous version of Eq. 101 ignoring the particular solution $U_p^{\pm}(\tau, \mu_i)$:

$$I_p^{\pm}(\tau, \mu_i) = \sum_{j=1}^{N} \left\{ C'_{jp} g'_{jp}(\pm\mu_i) e^{-k_{jp}(\tau - \tau_{p-1})} + C'_{-jp} g_{-jp}(\pm\mu_i) e^{-k_{jp}(\tau_p - \tau)} \right\}. \qquad (122)$$

Since $k_{jp} > 0$ and $\tau_{p-1} \leq \tau \leq \tau_p$, all exponentials in Eq. 122 have negative arguments as they should to avoid overflow in the numerical computations.